MACROPOROUS MATERIALS FROM SINTERING CAPPILARY AGGREGATE NETWORKS

by

Yutong Zhao

B.S. in Energy Engineering and Automation, South China University of Tech, 2015

Submitted to the Graduate Faculty of

Swanson School of Engineering in partial fulfillment

of the requirements for the degree of

Master of Science in Chemical Engineering

University of Pittsburgh

2017

UNIVERSITY OF PITTSBURGH

SWANSON SCHOOL OF ENGINEERING

This thesis was presented

by

Yutong Zhao

It was defended on

March 23, 2017

and approved by

Lei Li, PhD, Assistant Professor
Department of Chemical and Petroleum Engineering

Ian Nettleship, PhD, Associate Professor
Department of Mechanical Engineering and Materials Science

Thesis Advisor: Sachin Velankar, PhD, Associate Professor
Department of Chemical and Petroleum Engineering

MACROPOROUS MATERIALS FROM SINTERING CAPILLARY AGGREGATE NETWORKS

Yutong Zhao, M.S.

University of Pittsburgh, 2017

Capillary aggregate is one of the morphologies that appear in ternary mixtures of particles and two immiscible fluids. Capillary aggregates appear when two conditions are satisfied: the particles are fully-wetted by one of the two liquid phases, and furthermore, the wetting fluid has a volume fraction that is roughly equal to the particle volume fraction. Under these conditions, the wetting fluid creates highly compact particle aggregates called capillary aggregates. Recent research suggests that capillary aggregates can stick to one another to create a network in which capillary aggregates act as building blocks.

The aim of this study is to develop a macro-porous material from sintering capillary aggregate networks. In this study, morphologies of ternary mixtures in which the continuous phase is ethylene glycol, the wetting phase is light mineral oil and the solid phase is hydrophobic particles of low melting temperature polymer were studied. Capillary aggregate networks were prepared by suitable mixing methods, and then the mixtures were sintered to obtain macro-porous materials. Such macro-porous materials may be used as scaffolds for cells growth.

This thesis reported the implementation of capillary aggregate networks and the procedures of sintering and washing process. The effects of composition of ternary mixtures on porosity, pore sizes and number of aggregates were studied.

This study demonstrates that by sintering capillary aggregate networks, we can obtain high porosity materials with low particle loading, and obtain large pore sizes without using different size particles. Moreover, result shows that cells can grow well in the macro-porous materials.

DESCRIPTORS

Capillary aggregate network

Macro-porous material

Multiphase flow

Wet granular media

TABLE OF CONTENTS

LIST OF TABLES

LIST OF FIGURES

PREFACE

This thesis would not have been possible without the guidance and the help of several individuals who in one way or another contributed and extended their valuable assistance in the preparation and completion of this study.

First and foremost, Dr. Sachin Velankar, my advisor, under his guidance that I could complete this research works.

Junyi (Troy) Yang, always had kind concern and consideration regarding my academic requirements. He assisted me to finish the SEM images. I really appreciate his hardly work and advise.

Derrick Amoabeng, always here to help me and has been my inspiration and my good friend. He helped me to take SEM photos and finish the viscosity experiments.

Junyu (Anthony) Yang, for his unselfish and unfailing support.

Dr.Manju Singh from the Medicine School of the University of Pittsburgh, who assisted me on cells growth.

Dr.Joyita Banerjee, who assisted me on how to use experimental facilities.

My friends in the Chemical Engineering Department, who always give me some new ideas and moral support, I really appreciate it.

My parents and grandmother, who always encourage me when I met difficulties and supported my tuition without any doubts.

Yutong Zhao

1.0 INTRODUCTION

Ternary mixtures of particles and two immiscible fluids yield a wide diversity of morphologies [1]. The fluids may be water, oil, air, ionic liquids or highly viscous molten polymers and the particles sizes may range from less than 0.1 μm to 100 μm. The various morphologies result from an interplay between the preferential wettability of particles towards the two fluids, capillarity, and viscous forces encountered during mixing [1]. If the particles are fully wetted by one liquid, (i.e. the particles can be completely engulfed by one liquid phase), the various morphologies include pendular aggregates [2], funicular aggregates [3], capillary aggregates [2], particles-in-drop morphology [4] and drops-in-suspension [5] (i.e., where particles and drops of less wetting phase are independently suspended in the continuous wetting phase) [6,7]. If particles are partially wetted by both liquids, (i.e. morphologies of ternary mixture systems include Pickering emulsions [8], bijels [9], capillary state suspensions [10] and bridged emulsion gels. Second paragraph.

The specific morphology of interest to this thesis is capillary aggregates, i.e. clusters of particles that are bound together by a "single" body of the wetting fluid. They may be best regarded as drops of the wetting fluid that are highly filled with particles, often so highly filled that the particles protrude out of the drops. Capillary aggregates can either reside alone or stick to each other to create a capillary aggregate network in which capillary aggregates act as building blocks of the network. [11] This discovery might provide a convenient route to obtain

porous materials that can be processed readily. The previous research was conducted using silica particles and two immiscible highly viscous molten polymers to create capillary aggregate networks [11]. It would have been desirable to make the porous network permanent by sintering the particles together. However, due to the high softening temperature of silica, 2 the ternary mixtures obtained in the previous research were difficult to sinter. Thus, a permanent porous structure material was difficult obtain.

The main goal of this thesis is to implement capillary aggregate networks in ternary mixtures in which the continuous phase is water, and furthermore, replacing the silica particles with hydrophobic particles of low melting temperature polymer. In this way, it becomes easier to obtain dry macro-porous material by sintering the ternary system. The porous material may be used, e.g. as a scaffold for growing cells for tissue engineering.

Chapter 2 is the background and review of literature on granular material, capillary aggregate and capillary aggregate networks. Chapter 3 describes materials, and methods. The results and discussion of samples using two kinds of PE particles (with different molecular weight) are in Chapter 4 and 5. Chapter 6 is the conclusions.

2.0 BACKGROUND AND LITERATURE REVIEW

2.1 GRANULAR MEDIA WITH VARIOUS LIQUID CONTENT

2.1.1 Granular media

Granular materials are collections of macroscopic particles, like glass beads or sand.[12] Because of the macroscopic size of the particles, thermal effects and intermolecular forces effects can be ignored. The past few decades have seen enormous research on granular physics and media, but most studies, especially in the physics field, have focused on dry granular materials [12]. The dominant interactions of dry granular materials are inelastic collisions and friction, which are short-range and non-cohesive. One of the very common examples of dry granular material is the sand in desert. These are very dry and smooth particles and making tunnel through a sand pile is impossible. By adding a small amount of liquid, however, the mechanical properties of granular media can change in great deal. The main difference between dry and wet granular media is that wet granular media are cohesive due to surface tension and capillary effects of the liquid. For example, wet sand has much stronger structure than dry sand, people can make tunnels through wet sand pile like Figure 2.1 (b) or build sand castles using wet sand on beach.

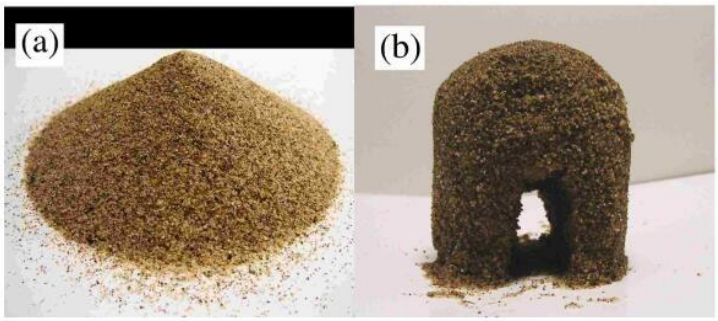

Figure 2.1 (a) Dry sand pile. (b) Wet sand pile with a tunnel**.** Reprinted with permission from Namiko, M et al. Copyright 2006 Taylor & Francis. [11]

2.1.2 Various states of granular media

In general, there are four states distinguished in wet granular media due to different liquid content as Figure 2.2 shows: [6,7]

(1) Pendular state: particles are held together by liquid bridges at their contact points.

(2) Funicular state: some pores are fully saturated by liquid, but there remain voids filled with air.

(3) Capillary state: all voids between particles are filled with liquid, but the surface liquid is drawn back into the pores under capillary action.

(4) Slurry state: particles are fully immersed in liquid and the surface of liquid is convex, i.e., capillary forces do not draw liquid back into the pores.

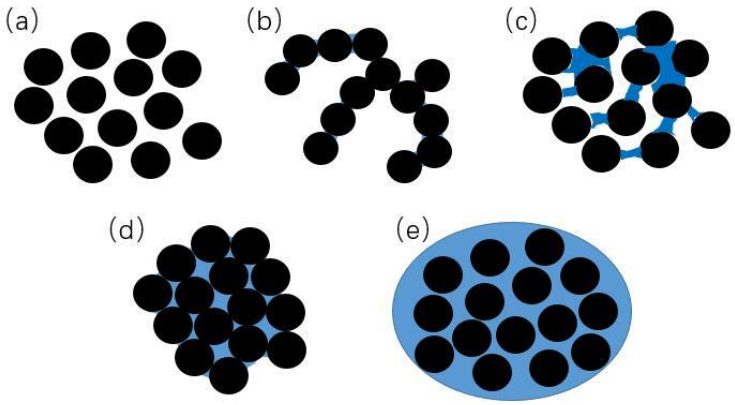

Figure 2.2 States distinguished in wet granular media due to various liquid content. (a) Dry granular media. (b) Pendular state. (c) Funicular state. (d) Capillary state. (e) Slurry state.

In the absence of liquid in a granular material, cohesion between particles is negligible. Cohesion arises in the pendular, funicular and capillary states [12]. Liquid content in pendular state granular media is quite small, and liquid bridges are formed at the contact points of grains. In pendular state, cohesive force only acts through these bridges. Wet granular media in funicular state has larger liquid content than that in the pendular state. Liquid bridges and liquid filled pores coexist, and both contribute to cohesive forces among particles. In the capillary state, granular materials are closed to being saturated, almost all pores are filled with liquid, but the liquid surface forms concave menisci. Because of capillary effects, pressure in the liquid menisci is lower than the air pressure. That pressure difference keeps all the particles residing in the liquid phase. Also, the suction gives rise to a strongly cohesive interaction among grains. In slurry state, the liquid pressure is equal to, or even higher than the air pressure, and the liquid urface becomes convex. No cohesive interaction exists among particles [12].

2.1.3 Ternary particle/liquid/liquid system

Ternary solid particle/fluid/fluid systems are soft materials that combine the physical properties of emulsions and suspensions, and which display unusual assembly phenomena connected to the interfacial activity of the particles [12] or to the capillary adhesion between the particles [3]. One advantage of the particle/fluid/fluid systems is the availability of a rich variety of parameters that enable tuning of their structure and assembly mode, such as material composition, fluids viscosities, particle wettability through surface chemistry modification, and particles size and shape.

In the past few decades, a lot of research on Pickering emulsion has been focused on systems composed of two immiscible fluids, often oil and water, with a small quantity of particulate species, such as particles with diameter of micron scale [13]. In Pickering emulsion field, these particles are partially-wetted by both fluids so that they adsorb at the interface between to fluids. This can introduce many interesting phenomena, such as particle-covered emulsion drops [14,15,16], particle-bridged drops [17,18,19,20,21] or bijels [22,23,24,25,37].

If particles can only be wetted by one of the fluid phases, however, they do not adsorb at the interface at all. The morphology of such systems is relatively complex and depends on the composition of three phases such as particle loading. Velankar research group has shown the rich phase behavior of ternary systems where the solid particles are highly wettable by one of the two fluid phases [2,3,13] in which case, percolation can either be induced by capillary bridging between the particles or by assembly of capillary clusters.

2.2 COHESION BETWEEN TWO PARTICLES

Wet sand on beach can be used to build sandcastle like Figure 2.1, because the particles can easily adhere to each other. The strong adhesion, which is named “capillary force”, is caused by liquid menisci, which form around the contact area of two adjacent particles. This cohesive force caused by surface tension and capillary effects has been taken into account in research fields of powders, soils and granular materials for a long time [26].

This mechanism is based on Young-Laplace equation as

$$\Delta P = P_a - P_l = \alpha[\frac{1}{r_1} + \frac{1}{r_2}] \qquad \text{Equation 2.1}$$

where ΔP is the pressure difference across the air-water interface, (sometimes called capillary suction), P_a is the air pressure, P_l is the liquid pressure, α is surface tension of the liquid-air interface and r_1 and r_2 are the curvature radii of the meniscus. As long as the curvature of the meniscus is positive, suction ΔP is positive.

For large particle sizes, another important parameter is the capillary length.

$$a = \sqrt{\frac{2\alpha}{\rho_l g}} \qquad \text{Equation 2.2}$$

which compares the capillary force caused by surface tension and gravity, where g represents the gravitational acceleration, ρ_l is the density of liquid and α is the surface tension.

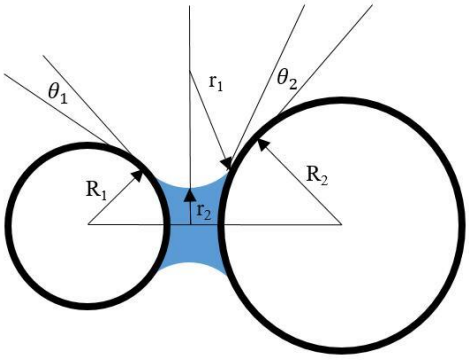

Figure 2.3 Schematic diagram of a liquid bridge between spherical particles.

Figure 2.3 shows two spherical particles with radius R_1 and R_2, respectively, r_1 and r_2 are the curvature radii of the meniscus. θ_1 and θ_2 is the contact angle and h is the distance between two spheres. If *h* is comparable or much greater than *a*, gravity will pull down the liquid, maybe even completely, and there will not a liquid bridge any more. However, for the relatively small particle sizes used in this thesis, gravitational effects can be neglected.

Considering two particles with radius R_1 and R_2, respectively, as shown on Figure 2.3, the cohesive force between two spheres due to liquid menisci is given by the sum of the surface tension and the suction [27]. Using Figure 2.3 again as an example, the capillary bridge force is

$$F_{bridge} = 2\pi\alpha R^* \left(cos\theta_1 + cos\theta_2 - \frac{D}{r} \right) \qquad \text{Equation 2.3}$$

where

$$R^* = \frac{R_1 R_2}{R_1 + R_2}$$

Capillary force can also be affected by surface heterogeneity (roughness), line tension, microscopic contact angle and surface deformation, et al. [6]

While this section is focused on pendular, i.e. pairwise, bridges between particles, what is important to this thesis is aggregation caused by multi-particle capillary interactions. That is discussed in the following section.

2.3 CAPILLARY AGGREGATE

When the particles are fully or almost fully wetted by the fluid, and if the wetting fluid volume fraction is comparable to that of particles, they will form a highly-concentrated combined phase, which behaves like a paste, which is called capillary aggregate. As shown on Figure 2.4, in a capillary aggregate, particles are packed tightly, and the aggregate cannot be easily broken due to strong capillary force binding particles together. The high yield stress of the paste-like phase also stabilizes the aggregate against breakup and coalescence.

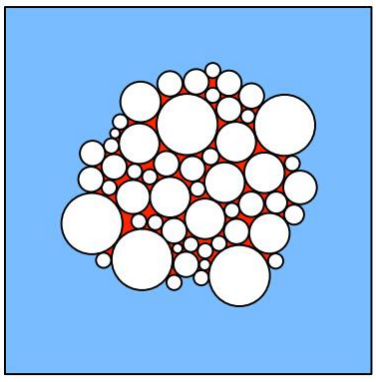

Figure 2.4 Capillary aggregate. Reprinted with permission from Demenech, T et al. Copyright 2014 Springer-Verlag Berlin Heidelberg. [12]

In the capillary aggregate, all the voids between particles are filled with wetting fluid, but the surface liquid is drawn back into the pores under capillary action [12]. The pressure in the aggregate is lower than the pressure outside in the wetting fluid, so the surface of wetting fluid is concave. The Laplace pressure difference, ΔP, keeps all particles packed with each other [28].

Previous articles from our group defined a quantity, ϱ as the ratio of the volume fraction of wetting fluid φ_w over the volume fraction of particles φ_p [2,29].

$$\varrho = \frac{\varphi_w}{\varphi_p} \qquad \text{Equation 2.4}$$

When ϱ is in a specific range, capillary aggregate clusters can form. For example, in the mixtures of silica particle with two immiscible polymers examined previously by Domenech and Velankar, capillary clusters forms after ϱ reaches 0.5 [11]. If ϱ is smaller than approximately 0.3, the aggregates are mostly pendular although occasional larger aggregates may appear. In the viscosity of $\varrho = 0.5$, the combined phase is jammed, i.e. the particle loading in the wetting fluid is so high that the combined phase has solid-like flow properties. Moreover, the particles are forced tightly into contact because the Laplace pressure in the wetting fluid is less than in the non-wetting fluid, as shown on Figure 2.4. At ϱ value exceeding about 1, the particles are no longer forced to remain in tight in contact. Instead, the combined phase consists of drops of the wetting fluid which themselves contain particles. Thus, the Laplace pressure wetting fluid equals or is higher than the pressure in the surrounding non-wetting fluid phase. The combined phase now behaves like “normal” liquid drops, and may either float to the top or sediment to the bottom of the non-wetting fluid phase depending on their density, and may readily coalesce into separate layer. [1]

Capillary aggregates have been known for a long time. Spherical agglomeration of particles, due to capillary aggregation by adding various amount of an immiscible second liquid which wets the particle, was firstly investigated and used in coal-cleaning industry to capture and upgrade fugitive fines to useful product coal [30]. In 1969, Sirianni, Capes and Puddington [31] reported that the process of removing particles from liquid suspension by selective wetting and agglomeration with a second immiscible liquid has many possible applications. By adding various amount of the particle-wetting liquid to an aqueous suspension of particles, the coal particles to be separated could be settled as flocs, as dense pellets or simply transferred to a continuous phase of the second liquid [31]. Capes and Darcovich [30] pointed out that spherical agglomeration, whereby these fines are preferentially wetted and agglomerated by oil mixed with the aqueous suspension of fine coal, provides perhaps the only practical method for upgrading extreme fines (tiny coal powders) to useful products on a large scale. Capes and Darcovich [30] also examined the main factors controlling the behavior of suspensions of fine particles to which a small amount of a second immiscible liquid was added, which includes: the free energy relationships at the liquid-liquid-solid interface; the amount of wetting liquid used in relation to the amount of solid and the type and intensity of mixing employed. In 1977, Sparks and Meadus [32] reported a means of size enlargement named spherical agglomeration process. In this process, particles suspended in a liquid are bonded together by a second liquid, which wets the solid surfaces and is immiscible with the suspending medium. With constant agitation, the capillary aggregates become spherical, this resulted in the continuous production of uniformly sized, highly spherical pellets. A systematic study of the effect of the main factors on the spherical agglomeration of chalcopyrite from mixture with pyrrhotite and a silica sand has been performed by House and

Veal [33]. Under certain circumstances, capillary aggregates can also be non-spherical [34, 35, 36]. In this study, we are more concerned about spherical capillary agglomeration.

In summary, spherical agglomeration was regarded as an excellent method to consolidate fine particles, or to separate them from a non-wetting fluid [33]. The relationship between stability of capillary aggregates and rheology has also been examined by Velankar research group. Heidlebaugh, et al, created capillary aggregates in the ternary system of silica particle/oil/water [13]. Figure 2.5 shows such systems at constant particle loading (20 wt%) with water content (wetting fluid) from 0 to 5 wt%. The continuous phase is oil, which does not wet the particles preferentially.

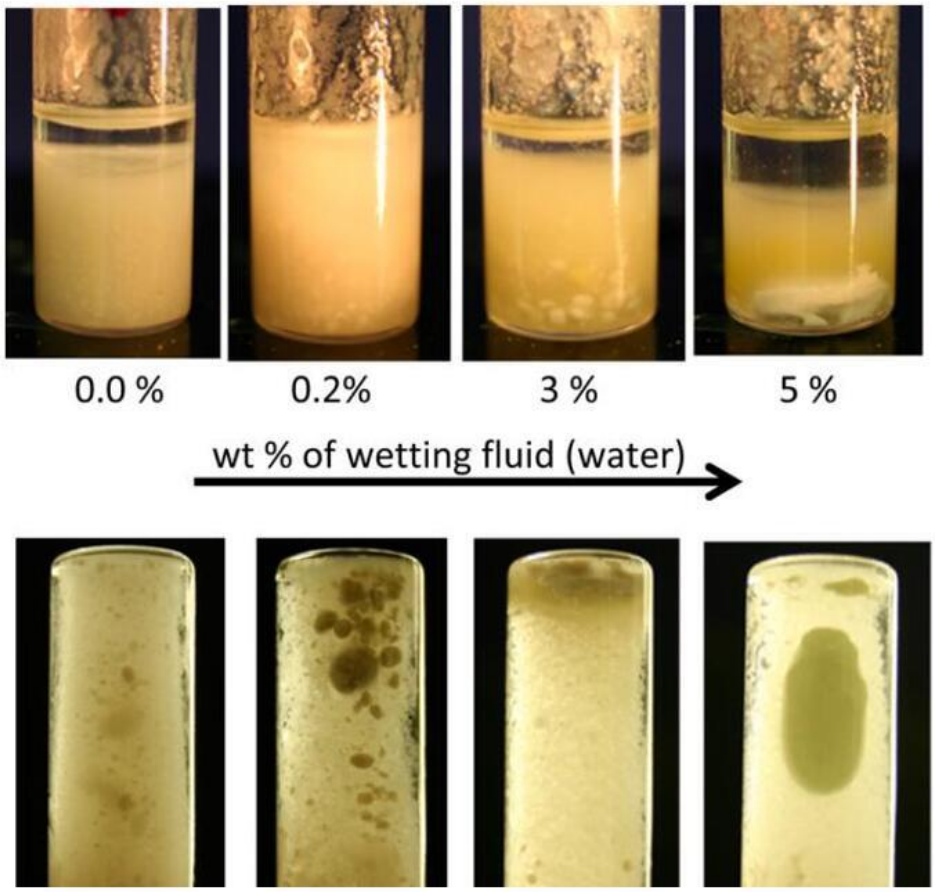

Figure 2.5 Silica particle/oil/water three phase system at increasing wetting fluid (water) content. Particle loading in all the five vials is 20 wt%. Bottom row shows the same vials as the top row but laid on the side and photographed from the bottom to show aggregates more clearly. Reprinted with permission from Heidlebaugh, S et al. Copyright 2013 American Chemical Society. [13]

At 20 wt% particle loading, the volume fraction of particles is only about 7.7%, whereas the particles are clearly occupying much more than the half of the vial as shown on the left most graph of Figure 2.5. This suggests these particles can form an attractive network in oil even when no water is added. By adding a very small amount of water, 0.2 wt%, sedimentation is completely eliminated indicating that a strong three-dimensional network has formed.

However, this is not a purely pendular network: confocal images shown in Figure 2.6 (a) and (b), show that at 0.2 wt% water content, a pendular network and capillary aggregates (marked by the yellow circle) both exist. By adding the water content to 5 wt%, both the number and size of capillary aggregates sharply increase and finally, at 5 wt%, a single large aggregate is formed.

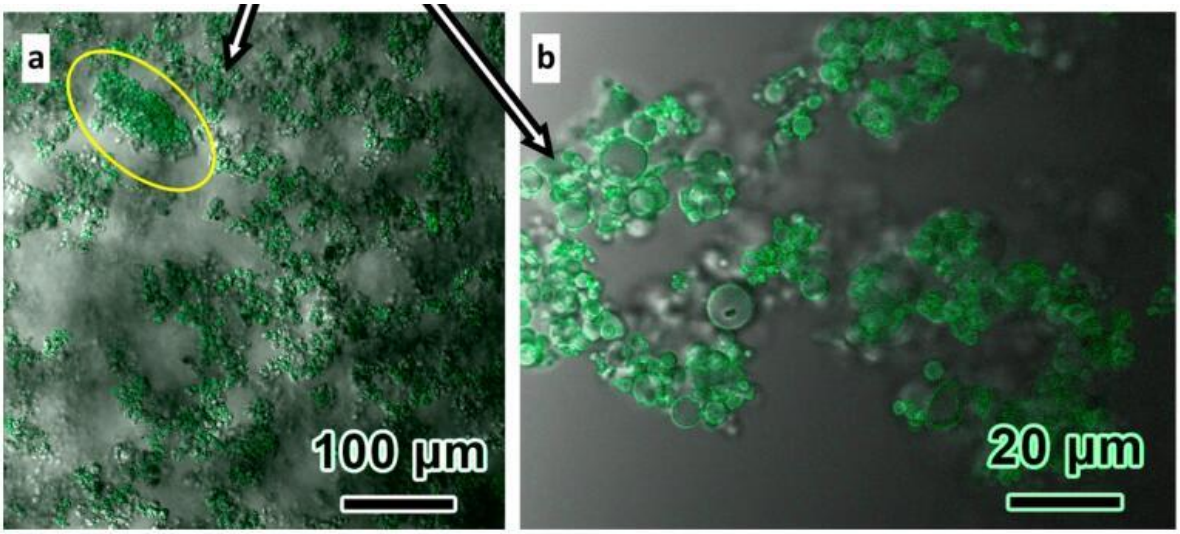

Figure 2.6 Confocal fluorescence images of vial at 0.2 wt% water content of Figure 9 under two different magnifications. Reprinted with permission from Heidlebaugh, S et al. Reprinted with permission from Heidlebaugh, S et al. Copyright 2013 American Chemical Society. [13]

The rheology of capillary aggregate clusters was also examined to understand why the aggregates are highly stable. Figure 2.7 shows the changes of viscosity with shear stress in the mixture of the same hydrophilic glass particles as in the previous two figures and water under various particle loadings.

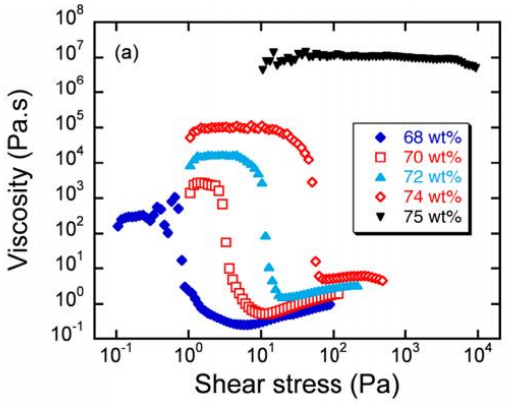

Figure 2.7 Viscosity measure during stress ramp experiments on particle-in-water suspensions for the 5 μm hydrophilic particles at various particles loading. Reprinted with permission from Heidlebaugh, S et al. Copyright 2013 American Chemical Society. [13]

As shown on Figure 2.7, at sufficiently high particle loading, the mixtures have a yield stress. Heidlebaugh, et al, suggested that it was this solid-like rheology that makes the capillary aggregates stable, resistant to both coalescence as well as breakup under mixing conditions.

2.4 CAPILLARY AGGREGATE NETWORK

It is notable that the spherical agglomeration process from the previous section was intended to separate particles from liquid suspension. However, in this thesis, we seek to use capillary aggregates as building blocks of a three-dimensional network.

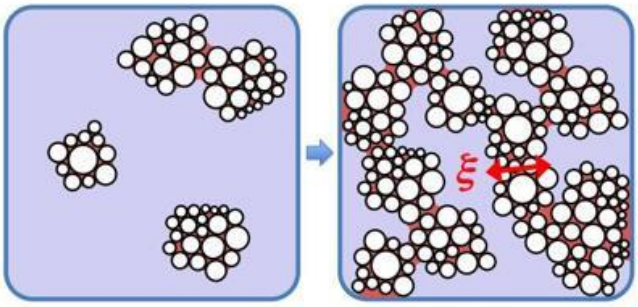

Figure 2.8 Two-dimensional schematic of capillary aggregate clusters network formation via compact capillary aggregation. Copyright 2014, Springer-Verlag Berlin Heidelbe Reprinted with permission from Demenech, T et al. Copyright 2014 Springer-Verlag Berlin Heidelberg. [11]

The capillary aggregates can either reside alone or stick to each other to create a capillary aggregate network when the combined phase loading $\phi_p + \phi_{wetting}$ is sufficiently high, as shown on Figure 2.8. The Velankar's research group focused on this interesting phenomenon, using mixtures of silica particle and two immiscible polymers. The non-wetting polymer was removed after sample preparation. All four of these samples have the same porosity, but by simply varying the ϱ value, different pore sizes can be realized.

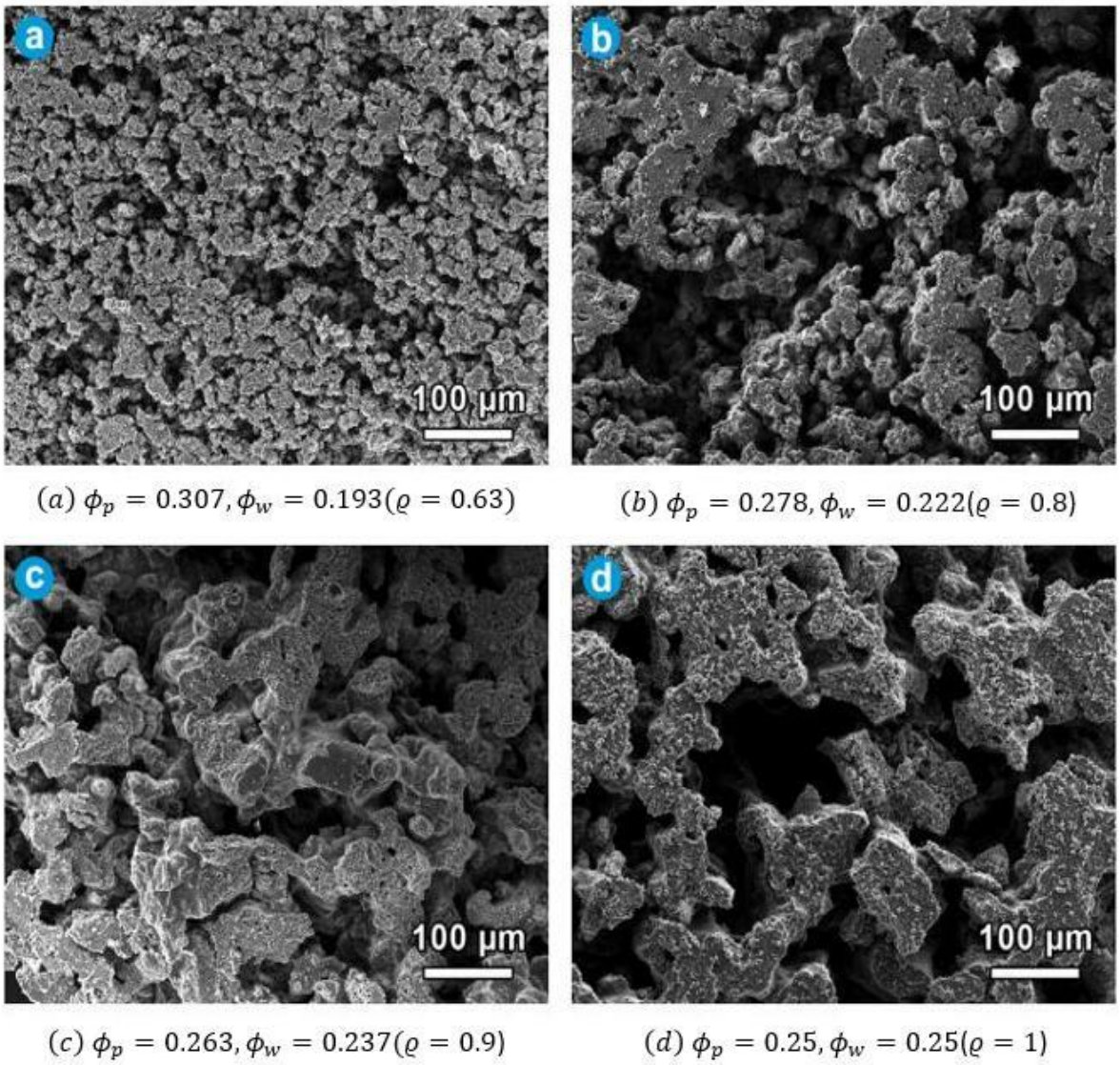

$(a)\ \phi_p = 0.307, \phi_w = 0.193 (\varrho = 0.63)$ $(b)\ \phi_p = 0.278, \phi_w = 0.222 (\varrho = 0.8)$

$(c)\ \phi_p = 0.263, \phi_w = 0.237 (\varrho = 0.9)$ $(d)\ \phi_p = 0.25, \phi_w = 0.25 (\varrho = 1)$

Figure 2.9 SEM micrographs of cut-out sections from co-continuous macro-porous solids showing in the change in domain size based on ternary composition: (a) $\phi_p = 0.307, \phi_w = 0.193\ (\varrho = 0.63)$; (b) $\phi_p = 0.278, \phi_w = 0.222\ (\varrho = 0.8)$; (c) $\phi_p = 0.263, \phi_w = 0.237\ (\varrho = 0.9)$; (d) $\phi_p = 0.25, \phi_w = 0.25\ (\varrho = 1)$ [11]

With volume fraction of wetting fluid which is comparable to the particle volume fraction, especially at $\varrho = 1$, pores with size on hundred-micron scale can be obtained. Such sizes are ideal for tissue-growth scaffolds since the size is large enough for cell migration growth. As mentioned at the end of previous section, the continuous capillary aggregate network results from partial coalescence of the capillary aggregate clusters due to their internal elasticity. The stability of this network (more specifically, the reason why it does not collapse under gravity or coarsen due to interfacial tension) is the solid-like behavior of the particle crowded phases [29]. In the combined phase of wetting fluid and particles with specific range of particle loading, at low shear stress, the viscosity is very high so that the mixture has a yield stress and does not flow readily.

2.5 MOTIVATION

In summary, the potential advantage of capillary aggregate networks is twofold. First, the building blocks of this network are not individually particles, but the aggregates. Thus, by varying the ϱ value, the pore sizes can be tuned without changing the particles. Second, the two-phase structure can be processed. For instance, prior to extracting one of the polymers from Figure 2.9 to make the porous structure, all the morphologies had two coexisting phases. Thus, they could have been "shaped", e.g. by extrusion or molding.

The previous research was conducted using silica particles to create capillary aggregate networks. Such particle networks are difficult to sinter because silica particles have relatively high softening point. Thus, the porous structure can only be maintained with the existence of both liquids, or by use of a wetting fluid that can be solidified, as shown on Figure 2.9. By using

low melting temperature particles, such as polyethylene, a sintering process can be readily implemented and dry macro-porous material can be obtained. Such material may be used as a scaffold for growing cells or for other applications where macro-porous morphology is desired. As polyethylene particles are hydrophobic, the ternary system in this thesis should be an inverted system compared to the ternary system reported by Heidlebaugh, et al. [11]. More specifically, the particles must be pre-dispersed in water or in a hydrophilic fluid, and then induced to aggregate by adding oil. The goals of this thesis are:

(1) Implementing capillary aggregate networks in mixtures that are inverted as compared to the mixtures of silica particles, oil and water by replacing hydrophilic silica particles by using hydrophobic polyethylene (PE) particles.

(2) Obtaining dry macro-porous material by sintering the ternary system mentioned above.

(3) Using that porous material as a scaffold for growing cells.

3.0 MATERIALS AND METHODOLOGIES

3.1 MATERIALS

Table 3.1 Materials used

Material	Diameter (μm)	Density (g/mL)	Melting point (℃)	Supplier
Micropoly 250S	2.0-4.0	0.97	129-131	MICRO POWDERS, INC
GUR 2122	8.0-20.0	0.93	130-135	Celanese
Light mineral oil		0.83		Fisher Scientific
Ethylene glycol		1.11		Fisher Scientific
Hexane		0.66		Fisher Scientific

3.1.1 Reason for using PE particles

The melting point of PE particles, which is around 130℃, is much lower than the softening point of silica particles. Thus, PE particles can be easily sintered. Also, PE particles are readily available in a variety of sizes. Finally, polyethylene is inert and hence if sintering proves

successful, the resulting porous materials may be well-suited for cell growth. Other possible candidates are polypropylene or latex polystyrene, or polymethyl methacrylate.

3.1.2 Reason for using glycol (rather than water) as the hydrophilic continuous phase

The first goal of this thesis is to implement capillary aggregate network in the mixtures that are inverted as compared to the mixtures of silica particles, oil and water by using hydrophobic PE particles. It is not advisable to pre-disperse particles in oil, and then add the hydrophilic fluid because the desired combined phase must be strong enough that capillary aggregates be stable.

Since the mixture of PE particles and oil must form a very sticky and strong paste, it would be difficult to disperse into the continuous phase once it was formed. Instead, PE particles must be pre-dispersed in a non-wetting continuous phase fluid, following by aggregating them by adding oil.

While it would be most reasonable to use water as the non-wetting fluid, this poses a significant problem: because of the high hydrophobicity of PE particles, it is impossible to maintain a stable suspension of PE particles in water. To illustrate that, a small amount of PE particles and water were placed in 6mL vials and were shaken in a vortex mixer for 45 seconds.

Figure 3.1 (a) GUR 2122 and water, 1min after shaking. (b) Micropoly 250S and water. 1 min after shaking.

Figure 3.1 shows that both GUR 2122 particle and Micropoly 250S particle cannot be wetted by water and instead form a film that sticks to the inner surface of vials. Because of this phenomenon, it is not possible to pre-disperse PE particles into water and then aggregate them with oil. Replacing water with ethylene glycol, however, solves this problem because ethylene glycol is found to wet the particles fully. Figure 3.2 shows that both GUR 2122 particles and Micropoly 250S particles can disperse well in ethylene glycol in a short time after being shaken in a vortex mixer. Although the mixtures in the vials in Figure 3.2 can also stratify after a long time, approximately 40 to 50 minutes, the suspension is stable for a sufficiently long time so that oil can be added and mixed well as described next.

Figure 3.2 (a) GUR 2122 and glycol, 5 min after shaking. (b) Micropoly 250S and glycol, 5 min after shaking.

3.2 MIXING PROCEDURE

The mixing procedures of ternary phase systems of polyethylene (either Micropoly 250S and GUR 2122) particle/glycol/oil is as follows:

(1) The desired quantity of glycol and PE particles were placed into a vial, then the closed vial was shaken in a vortex mixer for 45 seconds. This step yielded particles-in-glycol suspensions as shown on Figure 3.2.

(2) A small high-speed mixer called the Tissuemizer was used to further mix glycol and particles in the vial for 30 seconds.

(3) The desired quantity of oil was added by a syringe pump at a constant flow rate of 0.2 mL/sec. The oil was added by a syringe pump rather than a pipette because the syringe pump can give a relatively slow and constant flow rate and the oil can be added when the mixture is rapidly stirred by the Tissuemizer simultaneously. During the entire oil

addition process, the Tissuemizer was used to mix continuously so that the oil would be dispersed homogeneously. The Tissuemizer was switched off 30 seconds after all the oil was added. In contrast, adding the oil at once would cause rapid aggregation of the particles, and the formation of a strong and sticky particles-in-oil phase which is difficult to disperse homogeneously.

3.3 SINTERING PROCEDURE

3.3.1 Sintering procedure of Micropoly 250S particle/glycol/oil systems

The mixtures of Micropoly 250S, ethylene glycol and light mineral oil is runny and sticky so that these mixtures cannot be formed as pellets or extrudates. Hence, these mixtures must be sintered in the original container in which they are mixed.

As Micropoly 250S particles are relatively sensitive to temperature because of their low viscosity upon melting, sintering them at a temperature higher than the melting point causes flow and collapse of the porous structure, as will be discussed in Chapter 4. Thus, ternary phase systems of Micropoly 250S particles/glycol/oil were sintered in an oil bath heater, at 123℃ for 4 hours. Because such a long sintering time results in total evaporation of glycol in the samples, the samples were sintered in the closed 6mL vials.

3.3.2 Sintering procedure of GUR 2122 particle/glycol/oil systems

Sintering process of ultra-high molecular weight particles has been studied for a long time. [37,38] Hambir, S. and Jog, J.P. tested sintering two grades of ultra-high molecular weight polyethylene particles, Pilene Ultra 1900 and Stamylan UH 210. [39] Both grades of polyethylene particles were spherical. The diameters of both particles were in the range of 50-100 microns. The sintering behavior was studied using Leitz polarized light microscope equipped with hot stage. The measurements were carried out at five different isothermal temperatures in the range of 170-220 C° for six to ten minutes. They have also observed coalescence and recrystallization in both grades of particles.

Sintering of non-spherical high density polyethylene particles was studied by Torres, F.G., Cubillas, M.L. and Quintana, O.A. [40] In their experiments, the non-spherical PE particles were successfully sintered at 110-160 C° for two to eight minutes because of their lower melting point. It was reported that non-spherical particles reduce their surface area and adopt a more spherical shape. This influences the way coalescence between the particles takes place. In their study, the sintering process of non-spherical particles showed significant deviations from the tendencies predicted by the well-known and widely used Frenkel model. [41] The experimental results of Hambir et al suggest that it is possible to sinter ultra-high molecular weight particles even at temperature exceeding melting point. The well mixed mixture of GUR 2122 particles, ethylene glycol and light mineral oil is sufficiently strong that it can be either formed into pellets or extruded into strands. Pellets were prepared by placing the sample into a syringe with its front end cut off and troweling by a metal spatula. The cylindrical pellet then can

be ejected using the plunger of the syringe. Extrudates were prepared by placing the sample into an intact syringe then extruding the sample out without using a needle on the syringe.

3.4 PROCEDURE OF TAKING SEM IMAGES

Ethylene glycol and light mineral oil must be washed out of the sintered samples before SEM. Sintered samples were firstly washed by pure water for 24 hours, then were washed by hexane for 24 hours. Next the samples were dried in a fumehood for 8 hours.

The sintered samples which had been washed were then coated with platinum powders in vacuum.

The SEM images were taken by Scanning Electron Microscopy (SEM-JEOL JSM6510).

4.0 RESULT FOR MICROPOLY 250S PARTICLE/GLYCOL/OIL SYSTEMS

4.1 MICROPOLY 250S PARTICLES DISPERSED IN OIL

Figure 4.1 shows the Micropoly 250S PE particles dispersed in the light mineral oil. The left image was taken 1 minute after being shaken in a vortex mixer for 45 seconds, the right image was taken 1 minute after being mixed in the high-speed mixer (Tissuemizer) for 45 seconds.

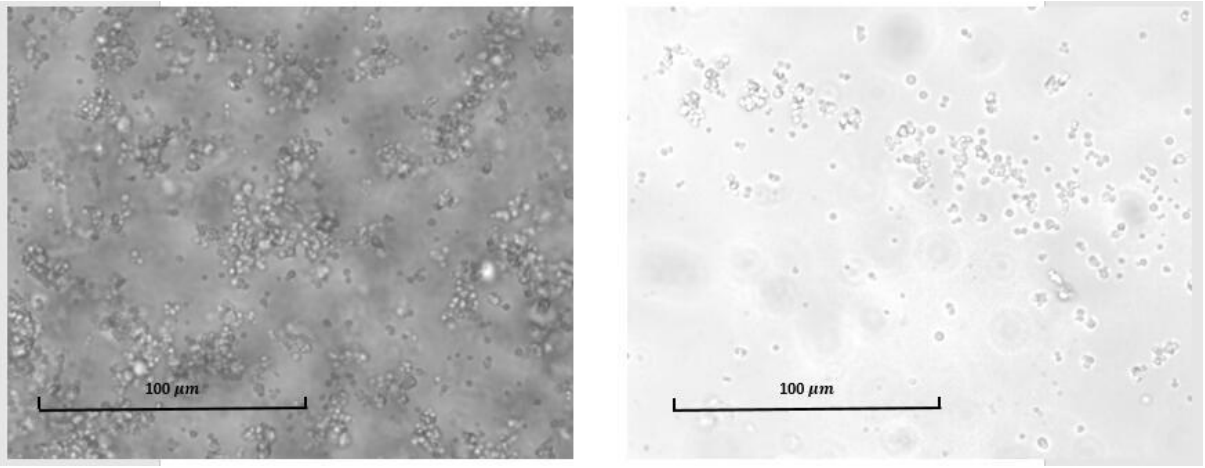

Figure 4.1 Micropoly 250S PE particles dispersed in light mineral oil (with a scalebar of 100 microns). The left graph was taken 1 min after being shaken in a vortex mixer for 45s; the right graph was take 1 min after being shaken in the Tissuemizer for 45s.

The Tissuemizer can give a higher shear rate so that the particles appear dispersed better in oil. The Micropoly 250S particles are nearly round with a diameter of few microns, in agreement with the diameter of 2 to 4 microns quoted by the manufacturer as shown on Table 3.1.

4.2 MICROPOLY 250S PARTICLE/GLYCOL/OIL SYSTEMS BEFORE SINTERING

Figure 4.2 shows microscopic images of Micropoly 250S particle/glycol/oil systems with various ϱ values. By increasing the ϱ value, the capillary aggregates increase in size consistent with the observations of Domenech from Figure 2.9 [11]. In order to take the images of Figure 4.2, the samples had to be squeezed between a glass slide and a coverslip and hence they were substantially damaged. However, macroscopic samples, e.g. as prepared in a vial may be regarded as macro-porous, i.e. if the glycol in the continuous phase can be removed while preserving the structure, one would obtain a porous structure with pore sizes on the scale of tens of microns.

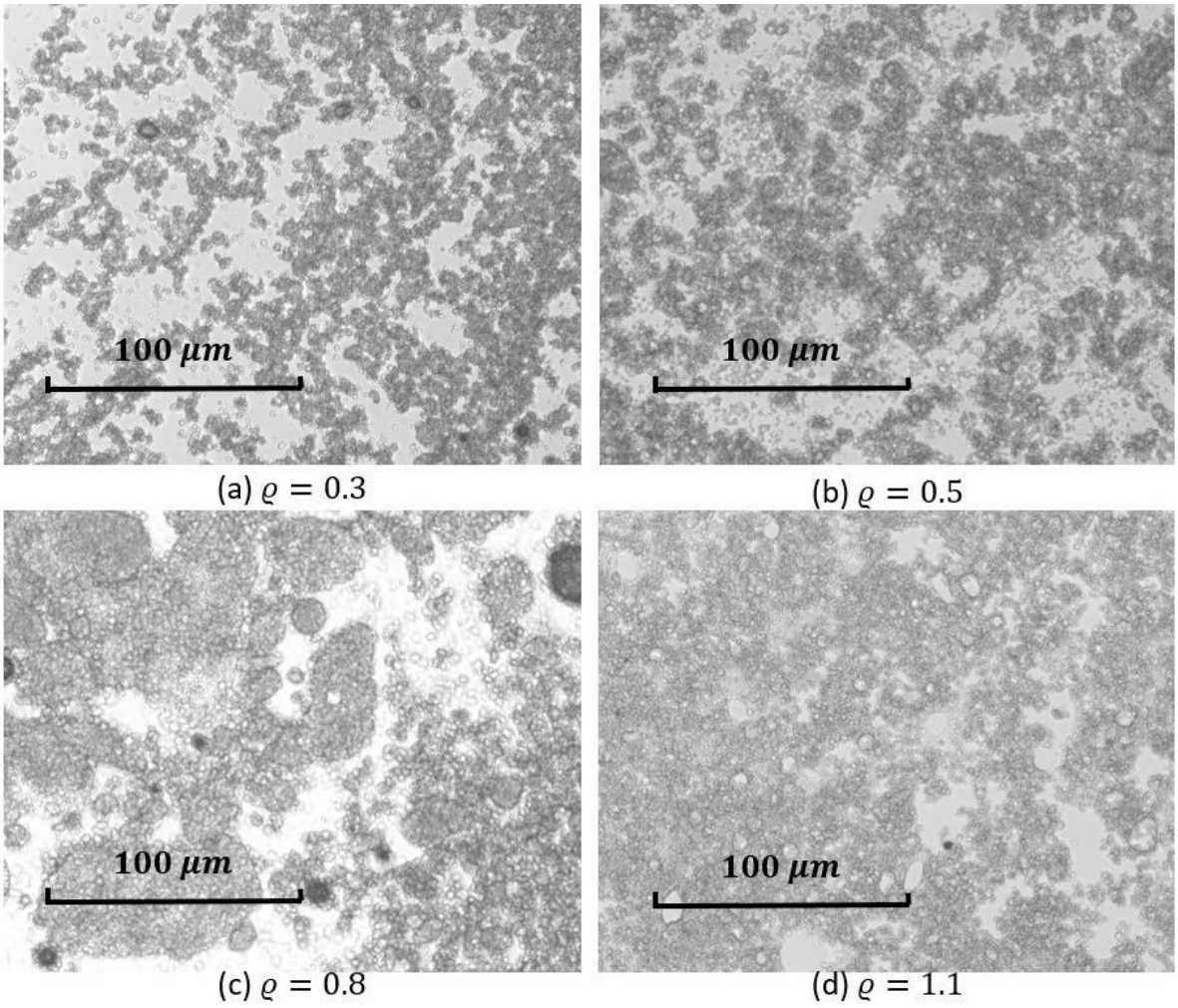

Figure 4.2 Optical microscopic images of Micropoly 250S particle/glycol/oil systems. (a) $\boldsymbol{\varrho = 0.3}$ (b) $\boldsymbol{\varrho = 0.5}$ (c) $\boldsymbol{\varrho = 0.8}$ (d) $\boldsymbol{\varrho = 1.1}$. For all the samples, $\boldsymbol{\varphi_{glycol} = 50\%}$.

When φ_{glycol} is in the range of 40% to 60%, the ternary mixtures were found to form relatively strong pastes, which could easily be sintered (as discussed later). If the φ_{glycol} is sufficiently large, however, the ternary mixtures were very runny, so sintering them while maintaining their structures proved impossible.

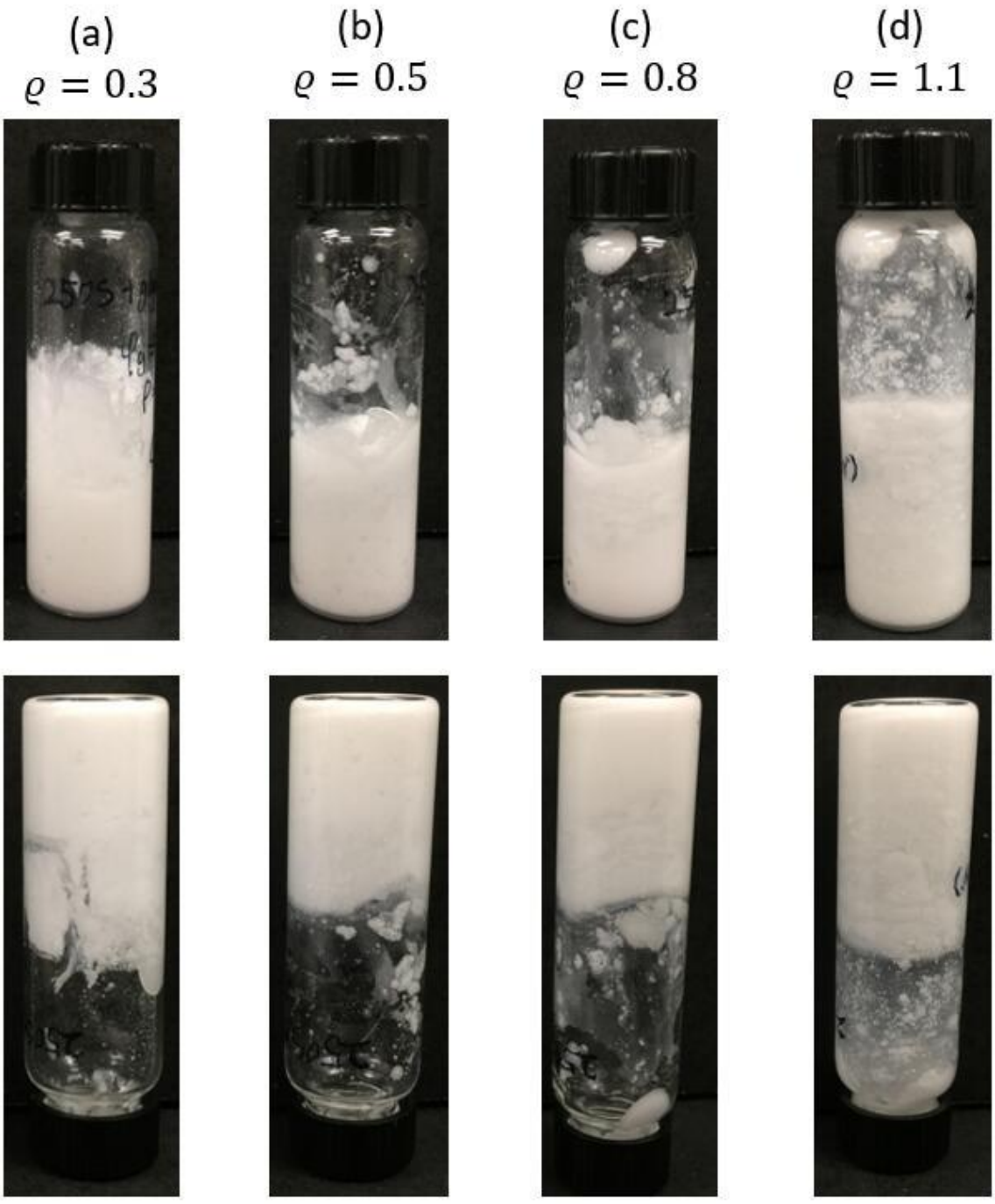

Figure 4.3 Micropoly 250S particle/glycol/oil systems prior to sintering. These samples have (a) $\boldsymbol{\varrho = 0.3}$ (b) $\boldsymbol{\varrho = 0.5}$ (c) $\boldsymbol{\varrho = 0.8}$ (d) $\boldsymbol{\varrho = 1.1}$. For all the samples, $\boldsymbol{\varphi_{glycol} = 50\ \%}$, thus the particle loading decreases from (a) to (d). The bottom row show the same vials as the top row, but upside down.

Figure 4.3 shows the ternary mixtures of Micropoly 250S particles/glycol/oil in vials before sintering. At high value of ϱ (i.e. $\varrho > 1.3$), the glycol separates, at least partially, from the oil/particle mixture, indicating that the target porosity of cannot be maintained. Compared to the silica particle/oil/water systems reported by Samantha Heidlebaugh, et al [11], where the separation occurs when the ϱ exceeds 0.875 (i.e. 7 wt% of water with 20 wt% of silica particles), the Micropoly 250S/glycol/oil systems can be maintained at a larger range of ϱ values. We acknowledge however the properties of such mixtures depend significantly on the mixing method and the mixtures of Heidlebaugh, et al were prepared by a vortex mixer, and not by a high-speed mixer as used in this study.

4.3 SELECTION OF TEMPERATURE AND TIME FOR SINTERING PROCESS

The goal of sintering is to bring the particles into a partially molten or flowing state so that particles in contact can bond to each other permanently. However, complete melting should be avoided since it may allow complete collapse, whereas we seek to preserve the macro-porous nature of the samples. Thus, precise control over sintering temperature and sintering time is critical. The melting temperature of Micropoly 250S particles is quoted by the manufacturer as 129℃ to 131℃. However, adding oil is likely to reduce the melting temperature of the sample. This was tested by first sintering the dry Micropoly 250S particles in a closed 6 mL vial in an oil bath at 125℃ for 4 hours. The particles remained unchanged, i.e. the sample remained a free-flowing powder of mostly single particles even after the annealing treatment. By adding a

small amount of oil (where volume of oil:particles = 0.2:1), however, the situation turned to be different. After heating in an oil bath at 125℃ for just 1 hour, the sample did not remain as separated single particles, but turned into a single porous lump, although it was not very strong and could be easily crumbled by a metal spatula. After 4 hours at 125℃, however, the structure collapsed completely and the sample became a semi-transparent single block which could not be crumbled easily by a spatula. This suggests that at 125℃, the particles (where volume of oil:particles = 0.2:1) are able to completely melt and flow, thus inducing complete collapse. Certainly, time ranges between 1 and 4 hours may be regarded as "optimal", however we instead sought to reduce the temperature to 123℃ to avoid complete melting. This was successful: the sample of Micropoly 250S particles and oil (where volume of oil:particles = 0.2:1) was heated at 123℃ for 4 hours, and the sample formed a very strong structure but did not collapse. A further decrease in temperature to 120℃ for 4 hours made the sample much weaker indicating insufficient melting.

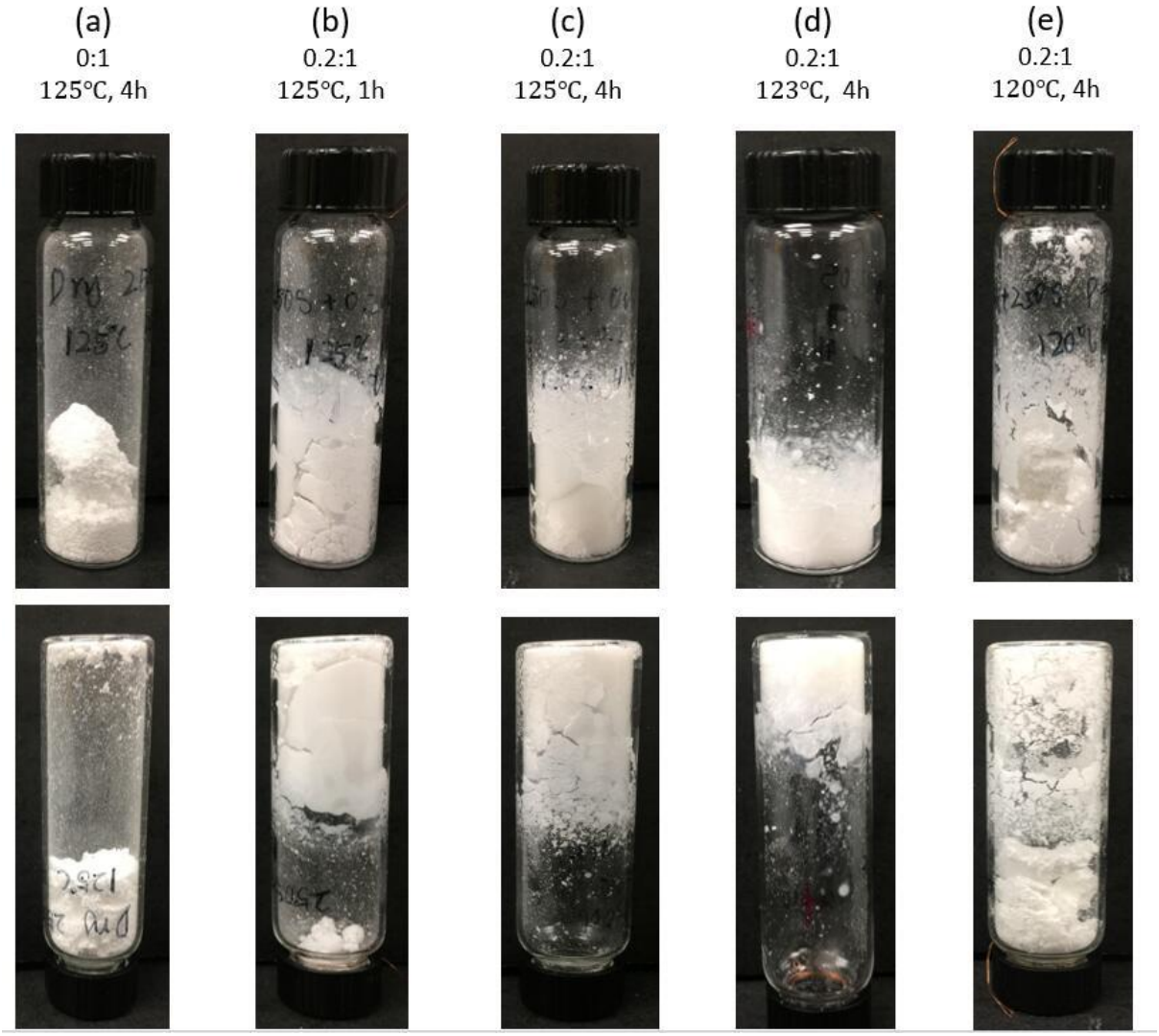

Figure 4.4 Sintering of Micropoly 250S particles at the conditions noted at the top. (a) No oil added. (b) oil : particles = 0.2:1. (c) oil : particles = 0.2:1. (d) oil : particles = 0.2:1. (e) oil : particles = 0.2:1. The bottom row show the same vials as the top row, but upside down.

Further increasing the volume fraction of oil may further lower the melting temperature of the mixtures. Samples of Micropoly 250S particles with oil:particle ratio of 0.7:1 and 1:1, respectively, were also tested by heating in the oil bath at 123℃ for 4 hours, as shown on Figure 4.5, and the results suggested that the levels of collapse increased with increasing the

volume fraction of oil, This was judged by the fact that by increasing the oil:particle ratio, the structure of the samples after heating become stronger. Also, the transparency of the heated samples increased by increasing the oil:particle ratio.

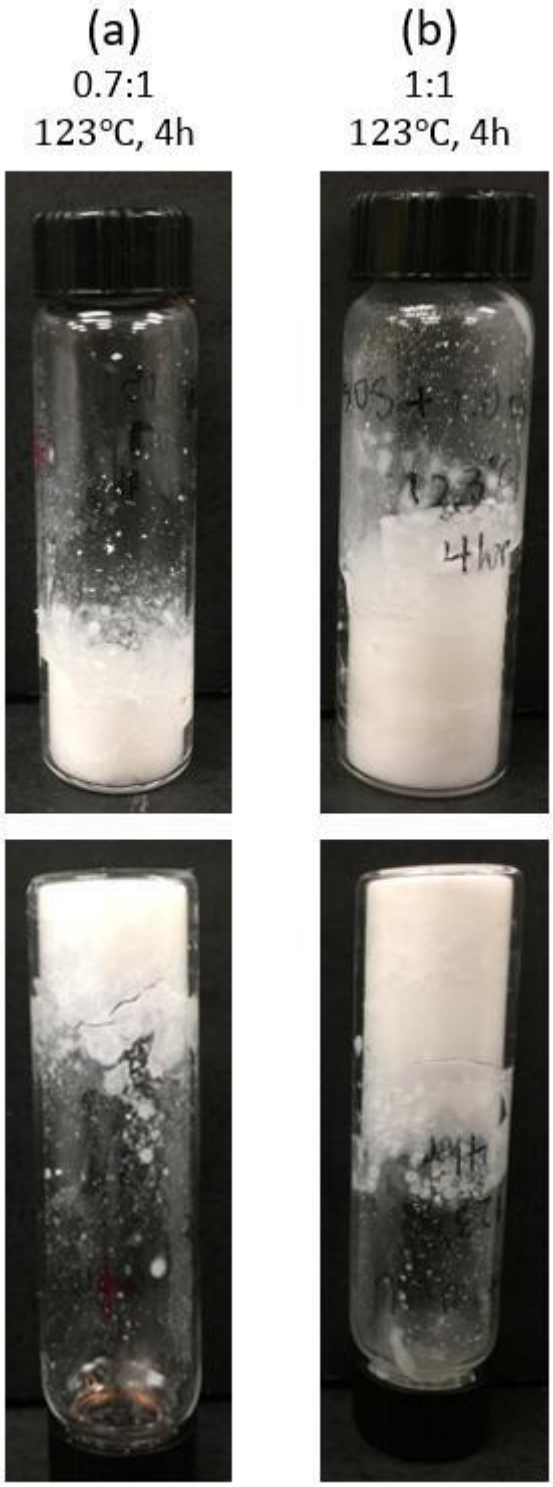

Figure 4.5 Sintering of Micropoly 250S particles at the conditions noted at the top. (a) oil : particles = 0.7:1. (b) oil : particles = 1:1. The bottom row show the same vials as the top row, but upside down.

Therefore, it is concluded that the sintering of Micropoly 250S particles is very sensitive to temperature, and moreover also sensitive to the amount of oil. Because the viscosity of molten Micropoly 250S particles is quite low, as will be described later, molten Micropoly 250S particles flow readily. Thus, there is only a narrow temperature range within sintering can be completed.

4.4 MICROPOLY 250S PARTICLE/GLYCOL/OIL SYSTEMS AFTER SINTERING AND WASHING

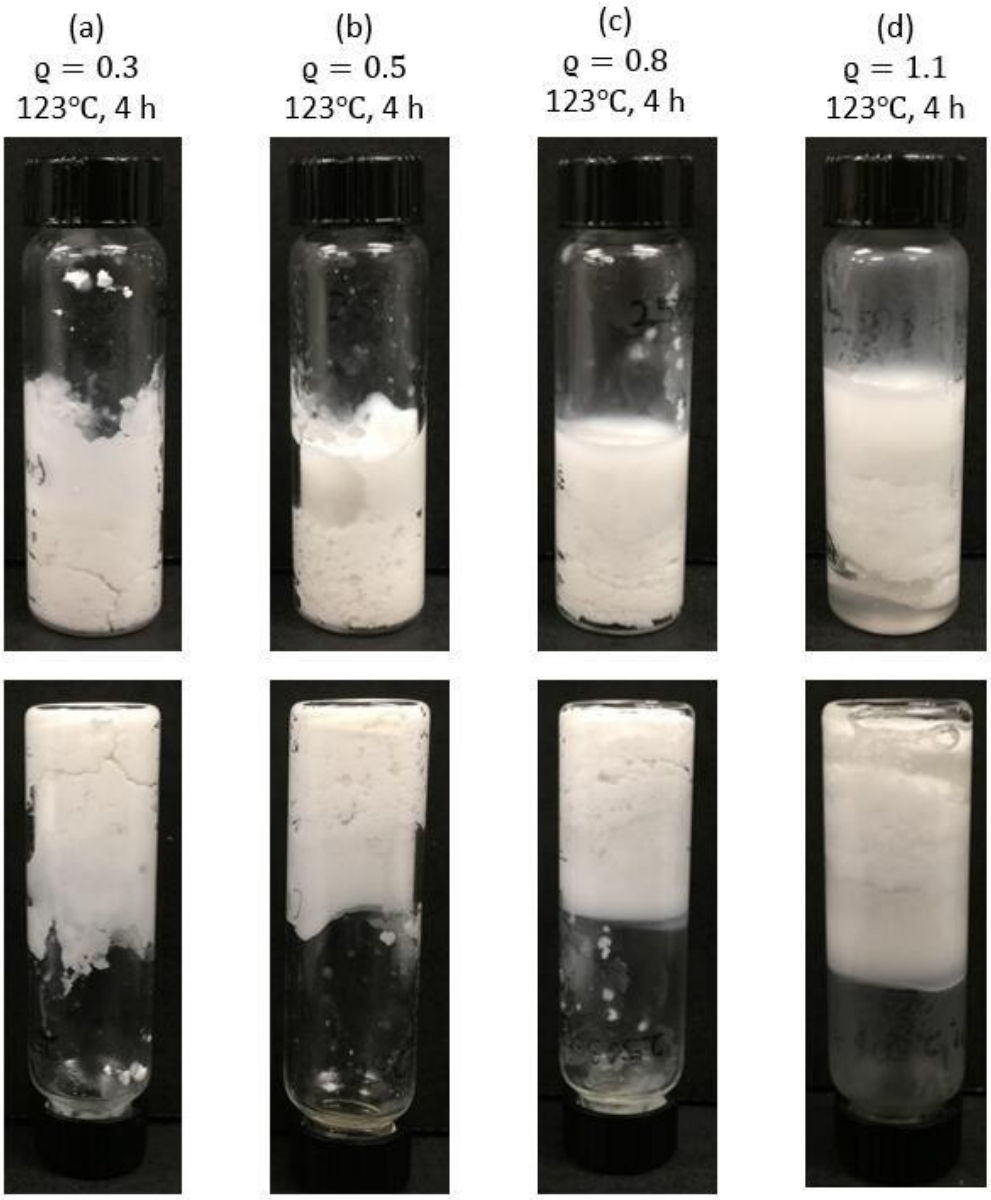

Figure 4.6 Sintering samples of Micropoly 250S particle/glycol/oil systems with various ϱ values at the conditions noted at the top. (a) $\boldsymbol{\varrho = 0.3}$ (b) $\boldsymbol{\varrho = 0.5}$ (c) $\boldsymbol{\varrho = 0.8}$ (d) $\boldsymbol{\varrho = 1.1}$. For all the sintered samples above, $\boldsymbol{\varphi_{glycol} = 50\%}$. The bottom row show the same vials as the top row, but upside down.

As shown on Figure 4.3, when the ϱ value is sufficiently large, at the bottom of all the vials, there was a clear layer of liquid which is the ethylene glycol that drained out of the mixture. Figure 4.6 shows that upon sintering, at high ϱ values, the height of the layer at the bottom increased, suggesting increasing levels of collapse of the macro-porous structure.

There are two possible reasons for this phenomenon: one is that in ternary phase systems, once the ϱ value exceeds about 0.5, yield stress reduces, the other is that the melting point reduces due to the increasing oil content. Both these can permit greater gravity-induced separation and collapse.

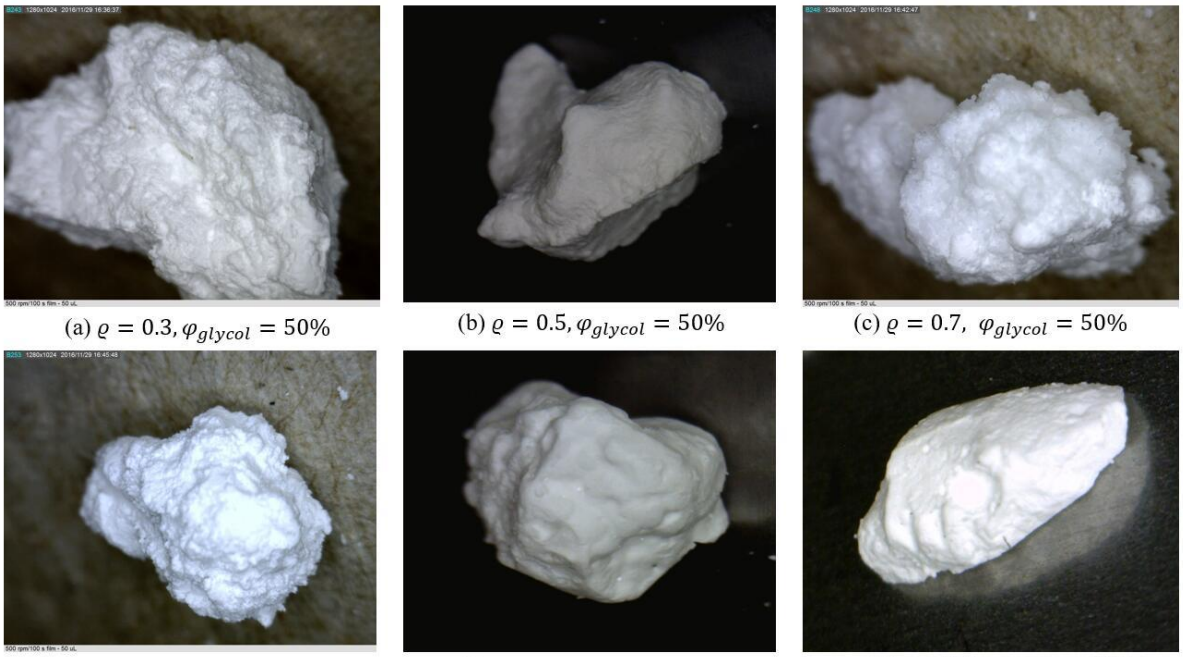

Figure 4.7 Images taken by Dinocam of samples of Micropoly 250S particle/glycol/oil systems with various ϱ value and volume fraction of glycol after sintering and washing. (The size of the samples is about 5 mm)

Figure 4.7 shows images taken at a relatively low magnification (using a “Dinocam” camera) of the samples of ternary phase mixtures of Micropoly 250S particles, glycol and oil, with various ϱ values and volume fractions of glycol, that have been sintered in an oil bath at 123℃ for 4 hours.

The size of all the six samples is approximately 5 mm. All the samples have been washed in water for 24 hours to remove the glycol, then in hexane for 24 hours to remove the mineral oil, and then dried in a fumehood for 8 hours. All these images show a bright white opaque appearance indicating a porous structure (in contrast, non-porous structures would appear translucent). We have also tried to use optical microscope to take the images (not shown) of the samples shown on Figure 4.7 on the magnification of 2.5 and 4 times. However, these images do not look very different from the photos of Figure 4.7.

Figure 4.8 shows the Scanning Electron Microscope (SEM) images at 500x magnification of samples of sintered ternary mixtures of Micropoly 250S particles, glycol and oil with various ϱ values. All the samples, with an original volume fraction of ethylene glycol of 50%, have been sintered in an oil bath at 123℃ for 4 hours and then washed in the same way as mentioned above.

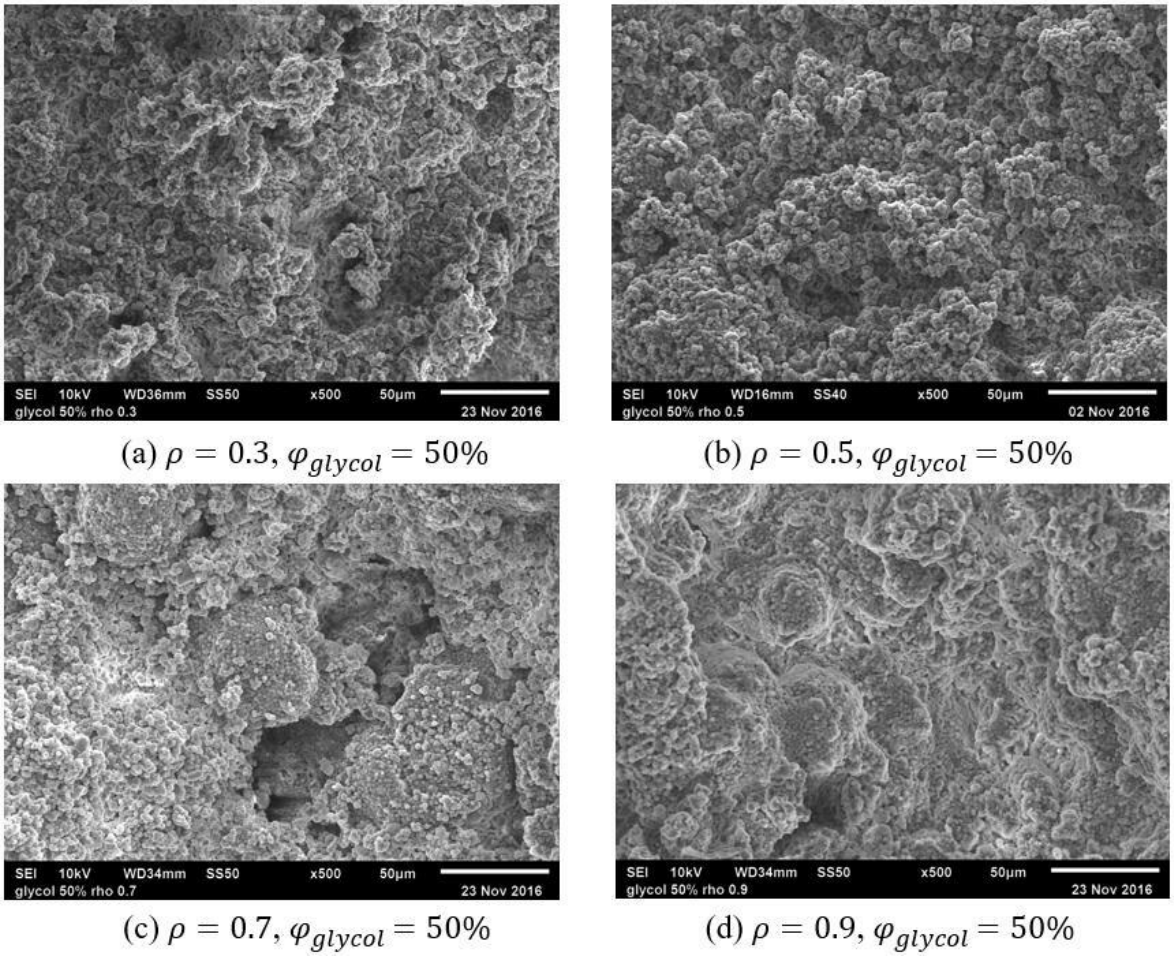

Figure 4.8 SEM images of sintered and washed samples of Micropoly 250S particle/glycol/oil systems with (a) $\boldsymbol{\rho = 0.3}$ (b) $\boldsymbol{\rho = 0.5}$ (c) $\boldsymbol{\rho = 0.7}$ (d) $\boldsymbol{\rho = 0.9}$. For all the samples, $\boldsymbol{\varphi_{glycol} = 50\%}$. The SEM magnification is 500x.

By increasing the ϱ value from 0.3 to 0.9, both number and size of capillary aggregates increases. Because for all the samples, the volume fraction of ethylene glycol is the same, the target porosity of the four samples should be the same. However, the glycol separation noted in Figure 4.6 suggests increasing levels of collapse of the structure. Thus, in fact, the porosity must be reducing as ϱ value increases, especially at ϱ = 1.1.

A low ϱ value, such as 0.3 and 0.5, the partial melting of the Micropoly 250S particles appears very slight and most of particles retain their initial shape. At higher ϱ values, especially at ϱ = 0.9, however, the particles appear more fused with each other, as shown on Figure 4.9, and many particles melted almost completely and then recrystallized upon cooling.

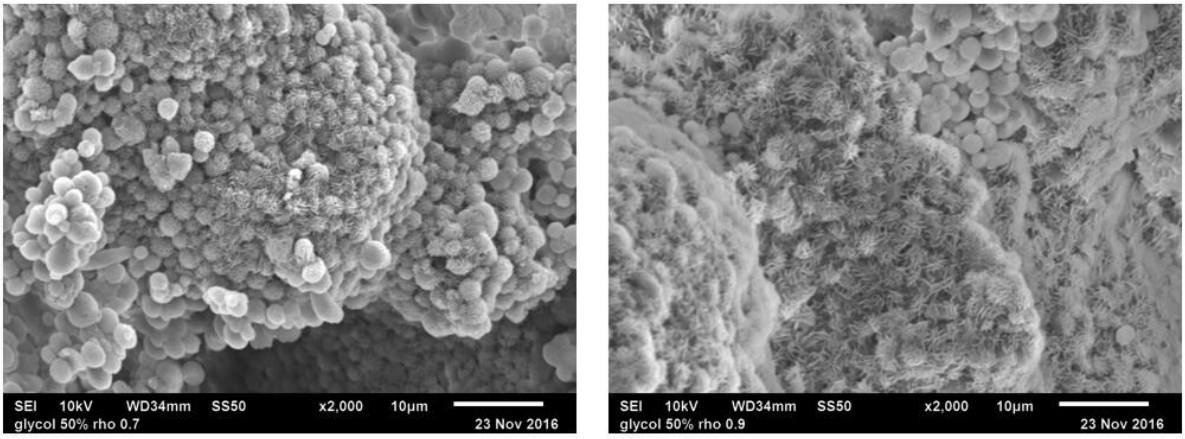

(a) $\rho = 0.7$, $\varphi_{glycol} = 50\%$ (b) $\rho = 0.9$, $\varphi_{glycol} = 50\%$

Figure 4.9 SEM images of sintered and washes samples of Micropoly 250S particle/glycol/oil systems with (a) $\boldsymbol{\rho = 0.7}$ (b) $\boldsymbol{\rho = 0.9}$. For both samples, $\boldsymbol{\varphi_{glycol} = 50\%}$. The SEM magnification is 2000x.

The recrystallization of spherical particles was also realized by Hambir, S. and Jog, J.P. coalescence of two spherical particles can be described by a simple theoretical model developed by Frenkel. [41] He explained the welding of two spheres by Newtonian viscous flow with by equating the change in the surface free energy with the viscous dissipation resulting in the following equation:

$\frac{x^2}{a} = \frac{3}{2}\gamma\frac{t}{\eta}$	**Equation 4.1**

Where, x is the neck radius, a is the initial radius of the spherical particle, γ is the surface tension and η the viscosity of the medium. The model assumes that the coalescence occurs by mutual inter-penetration of molten chains and the radius decreases since the volume of the two incompressible particles is constant. The level of coalescence was described by the variation x^2/a.

4.5 VISCOSITY OF MOLTEN 250S PARTICLES

The viscosity of molten Micropoly 250S particles was measure by an AR2000 advanced rheometer at 150℃. The gap was set to be 500 microns, and the sample's viscosity was tested under the shear stress of 10, 20 and 30 Pa respectively.

From the data, the viscosity of molten Micropoly 250S particles was considered to be about 1.5 Pa*s. As the viscosity of Micropoly 250S particles is such a low value, the particles are quite easy to flow when completely melting. Thus, the sintering procedure of Micropoly 250S samples is strict: to make it partially melting, the sample can only be sintered at the temperature slight lower than the melting point for a long time, but the temperature should not be too low, otherwise the particles will not melt. In summary, the sintering temperature is very narrow.

5.0 RESULTS FOR GUR 2122 PARTICLE/GLYCOL/OIL SYSTEMS

5.1 INITIAL AGGREGATION OF GUR 2122 PARTICLES

Figure 5.1 shows GUR 2122 particles dispersed in light mineral oil and in ethylene glycol. Both mixtures were mixed by high-speed mixer (Tissuemizer) for 1 minute.

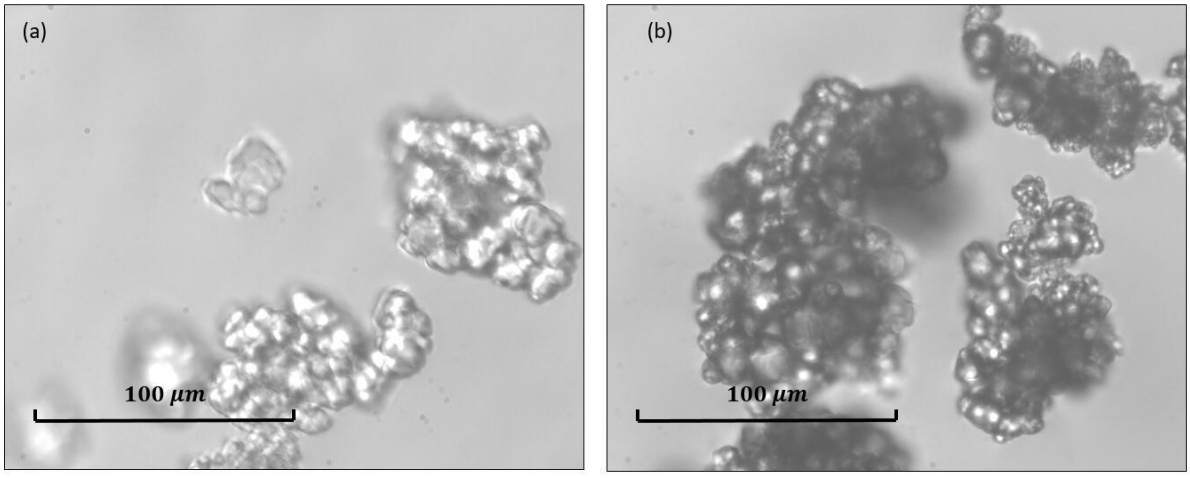

Figure 5.1 (a) GUR 2122 particles dispersed in oil. (b) GUR 2122 particles dispersed in ethylene glycol.

As shown on Figure 5.1, the GUR 2122 particles are initially aggregated, forming "popcorn-like" clusters, approximately 50 to 100 microns in size. This immediately suggests that the behavior of ternary systems based on these particles will be more complex than for the Micropoly 250S

microparticles. This is because for spherical particles such as Micropoly 250S, a ϱ value of approximately 0.5 marks the appearance of capillary aggregates. At ϱ value much smaller than 0.5, there is not sufficient oil for engulfing all particles. At much larger ϱ values, the combined phase lacks sufficient yield stress to stabilize capillary aggregate networks. For non-spherical particles such as GUR 2122, however, the ϱ values needed for aggregation may be significantly different.

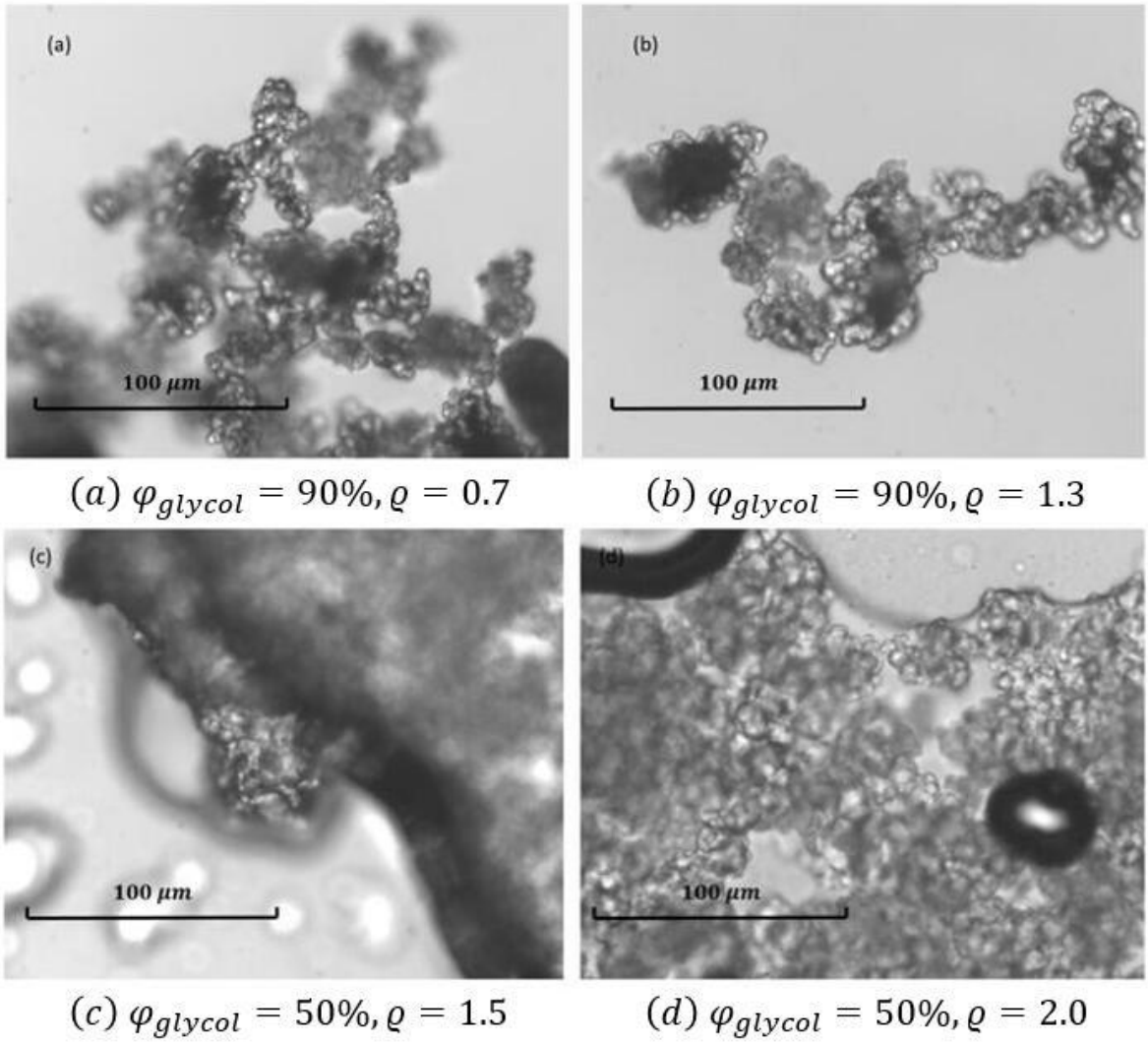

Figure 5.2 Optical microscopic images of GUR 2122 particle/glycol/oil ternary systems before sintering with (a) $\boldsymbol{\varphi_{glycol} = 90\%, \varrho = 0.7}$ (b) $\boldsymbol{\varphi_{glycol} = 90\%, \varrho = 1.3}$ (c) $\boldsymbol{\varphi_{glycol} = 50\%, \varrho = 1.5}$ (d) $\boldsymbol{\varphi_{glycol} = 50\%, \varrho = 2.0}$

This is illustrated by Figure 5.2 which shows ternary mixtures of GUR 2122 particle, glycol and oil. Despite the large difference in ϱ value between the images (a) and (b) in Figure 5.2, the appearance of the aggregates is similar, and moreover both resemble Figure 5.1. Especially, in Figure 5.2 (b), the volume fraction of oil is even larger than the volume fraction of the particles, and for spherical particles, a slurry state would be expected. In contrast, in Figure 5.2 (b), the oil

does not appear to encapsulate the particles and therefore this is definitely not a slurry state. This suggests that these aggregates are not capillary aggregates but similar to the initial "popcorn-like" aggregates of GUR 2122 particles, but now incorporating oil. When the ϱ value is sufficiently large (much larger than explored in the previous chapter), as shown on Figure 5.2 (c) and (d), the situation changes: all the particles are incorporated into the oil and there is also large-scale separation as can be seen on Figure 5.3.

Figure 5.3 shows ternary mixtures of GUR 2122 particles, glycol and oil prior to sintering. As may be expected, the samples became "runnier" with increasing the ϱ value, and when the ϱ value exceeded 1.3, separation of particles and oil occurred suggesting that the values exceeding 1.3 are not suitable for sintering.

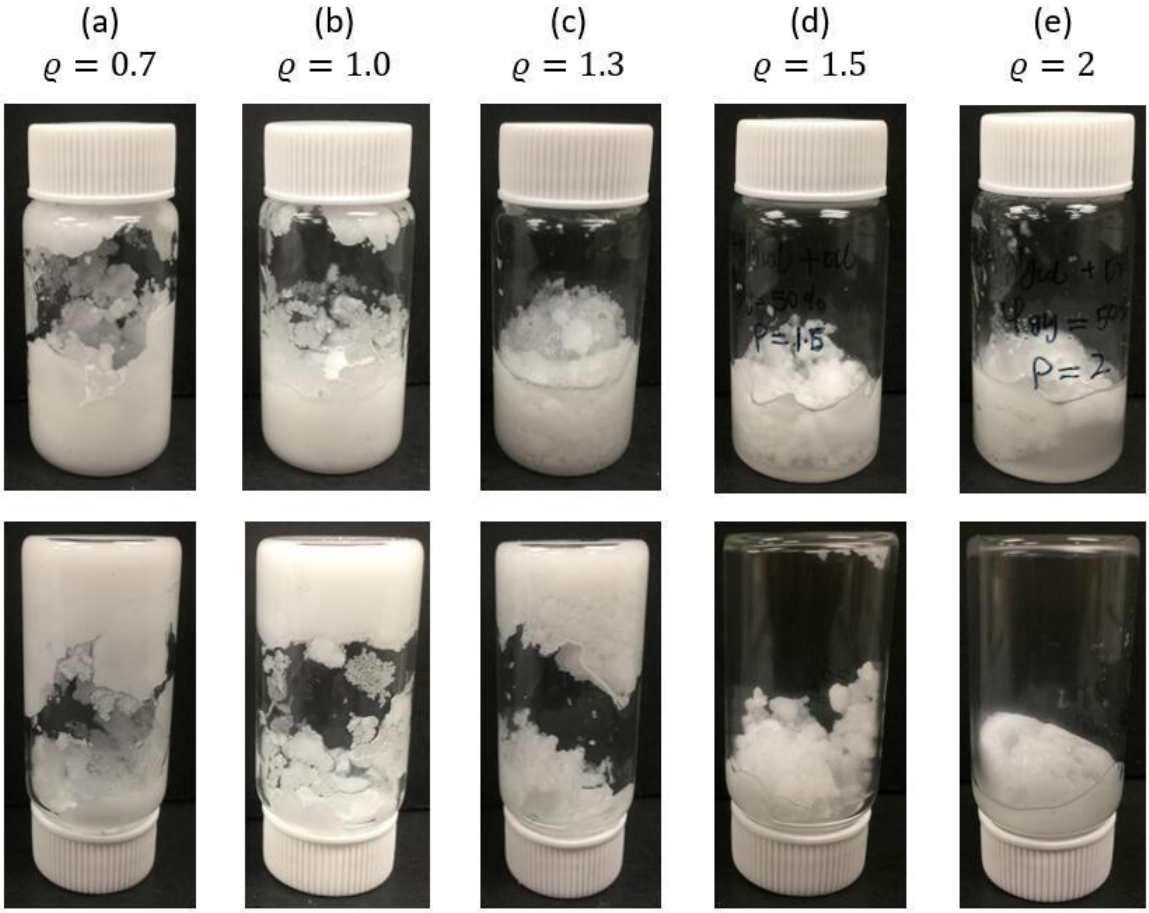

Figure 5.3 Not sintered GUR 2122 particle/glycol/oil systems with (a) $\boldsymbol{\varrho = 0.7}$ (b) $\boldsymbol{\varrho = 1.0}$ (c) $\boldsymbol{\varrho = 1.3}$ (d) $\boldsymbol{\varrho = 1.5}$. (e) $\boldsymbol{\varrho = 2}$. For all the samples, $\boldsymbol{\varphi_{glycol} = 50\%}$. The bottom row show the same vials as the top row, but upside down.

5.2 SELECTION OF TEMPERATURE AND TIME FOR SINTERING PROCESS

Molten GUR 2122 particles have much higher viscosity than molten Micropoly 250S particles. Indeed, it is well-known that ultra-high molecular weight polyethylene (UHMWPE) does not flow readily, and is generally considered to have gel-like flow properties. We attempted to

measure the viscosity of molten GUR 2122 particles, but were unsuccessful even in molding disc-shaped samples for rheological testing. As shown on Figure 5.4, a conventional compression molding operation led to highly porous samples because GUR 2122 particles do not flow sufficiently (even when completely molten) to completely consolidate.

Figure 5.4 Conventional compression molding operation for disc-shaped sample of molten GUR 2122

Hence, the time and temperature of the sintering process of GUR 2122 samples does not need to be controlled as strictly as the sintering process of the Micropoly 250S samples. Sintering at a temperature significantly higher than the melting point of GUR 2122 particles for a short time should be sufficient for sintering.

Figure 5.5 (a) and (b) show the sintered sample of the dry GUR 2122 particles and the mixture of oil and GUR 2122 particles in a 0.2:1 ratio. After sintering at 150℃ for 10 minutes, both samples were fairly strong and formed a single porous block. Figure 5.5 (c) shows the mixture of oil and GUR 2122 particles in a 0.2:1 ratio, sintered at the same temperature but for two hours. That sample is quite similar to Figure 5.5 (b), but stuck to the inner surface of the vial. It is noteworthy that this temperature far exceeds the melting temperature of polyethylene, i.e., even keeping the samples fully molten for two hours did not cause collapse. This confirms, the sintering time is not very important: the high viscosity of GUR 2122 samples ensures that the porous structure will not collapse under gravity making sintering much easier.

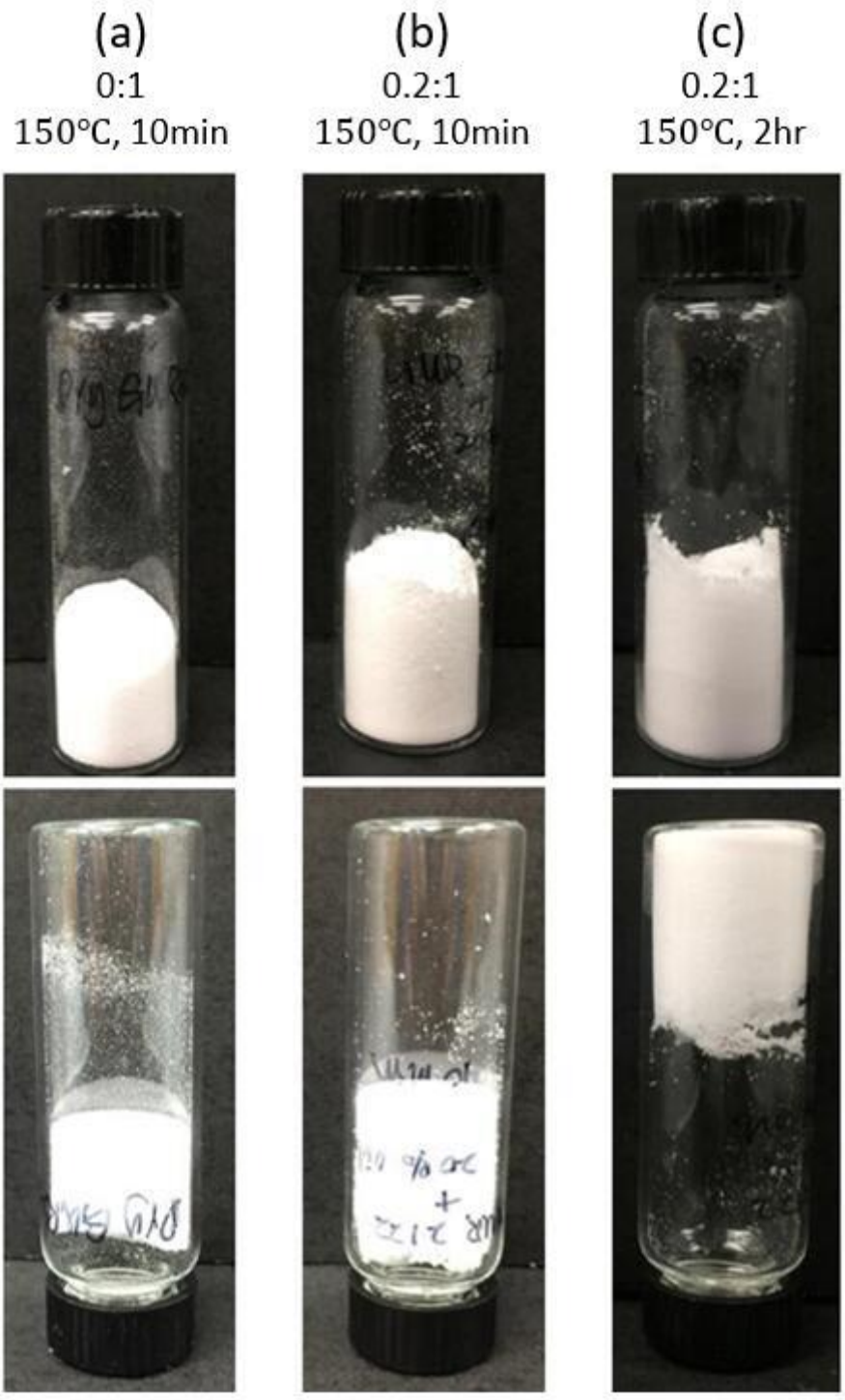

Figure 5.5 Sintering of GUR 2122 particles at the conditions noted at the top. (a) No oil added (b) oil: particle = 0.2:1. (c) oil: particle = 0.2:1. The bottom row show the same vials as the top row, but upside down.

Further increasing the volume fraction of oil may also further lower the melting temperature of the mixtures of GUR 2122 particles and oil. Samples of GUR 2122 particles with oil : particles ratios of 1:1 and 2:1 were also tested by sintering in the lab oven for 2 hours, as shown on Figure 5.6. When a lot of oil was added, for example Figure 5.6 (b), the sample became a semi-transparent block indicating a complete loss of porosity since the particles were fully-engulfed by oil.

What is notable is that the oil dissolved completely in the molten GUR 2122 particles. It was found that for the sample of Figure 5.6 (b), for which the oil volume fraction is very large, after sintering only very small amount of oil came out of the sample. The explanation of this phenomenon could be that particles absorbed the oil, and when the polymer recrystallized, the oil simply was retained in the amorphous portion of the semi-crystalline sample.

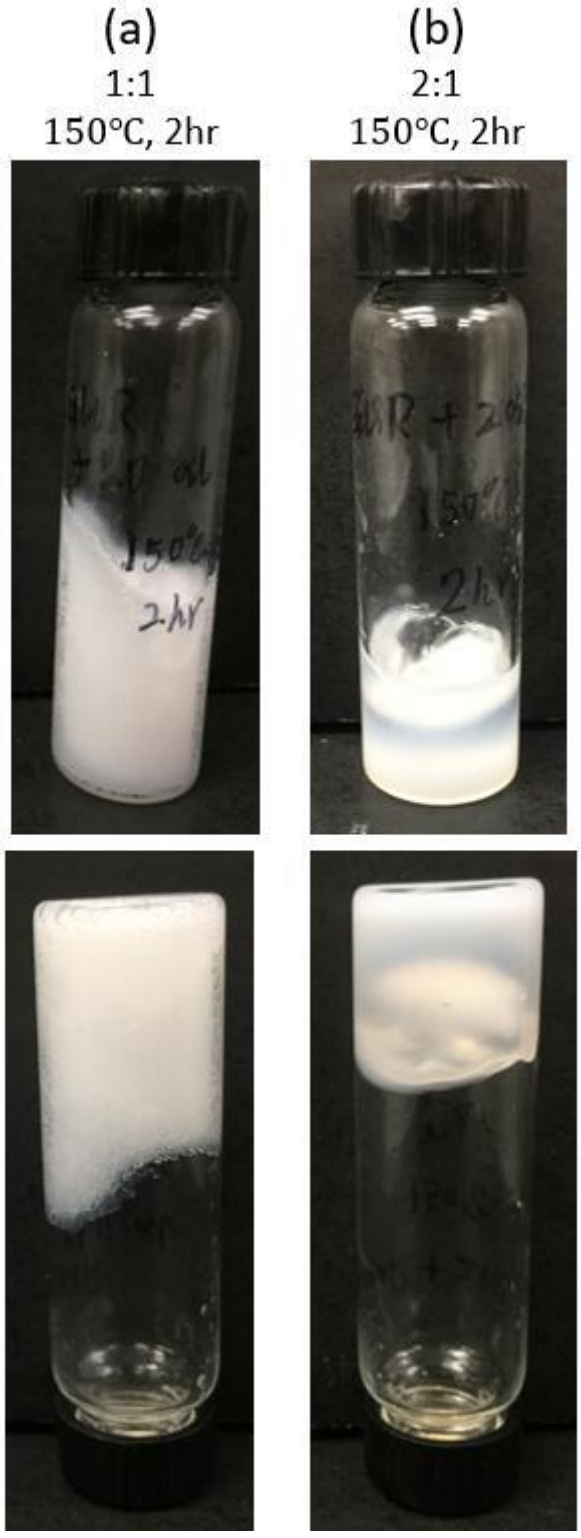

Figure 5.6 Sintering of GUR 2122 particles at the conditions noted at the top. (a) oil: particle = 1:1. (c) oil: particle = 2:1. The bottom row show the same vials as the top row, but stand upside down.

Ternary mixtures of GUR 2122 particles, glycol and oil were found to be much stronger (prior to sintering) than corresponding to ternary mixtures of Micropoly 250S particles, glycol and oil. In fact, they could be shaped, e.g., formed into either pellets or extrudates, as shown on Figure 5.7 and Figure 5.11. Thus, instead of sintering in the original vials, they were sintered in the form of pellets and extrudates in a foil pan containing glycol at 150℃ for 10 minutes, using a lab oven. Pellets and extrudates floated on the surface of the glycol in the foil pan. Due to the excess glycol, and the much shorter sintering time, glycol evaporation was not a significant problem.

5.3 PELLETS OF THE GUR 2122 PARTICLE SAMPLES AFTER SINTERING AND WASHING

Pellets of the mixture of GUR 2122 particles, glycol and oil were prepared by placing the ternary mixture into a syringe with its front end cut off and troweling with a metal spatula. The cylindrical pellet was then ejected using the plunger of the syringe, as shown on Figure 5.7 (a) and (b). Figure 5.7 (c) shows the pellets after sintering and washing in water for 24 hours to remove glycol and in hexane for 24 hours to remove oil.

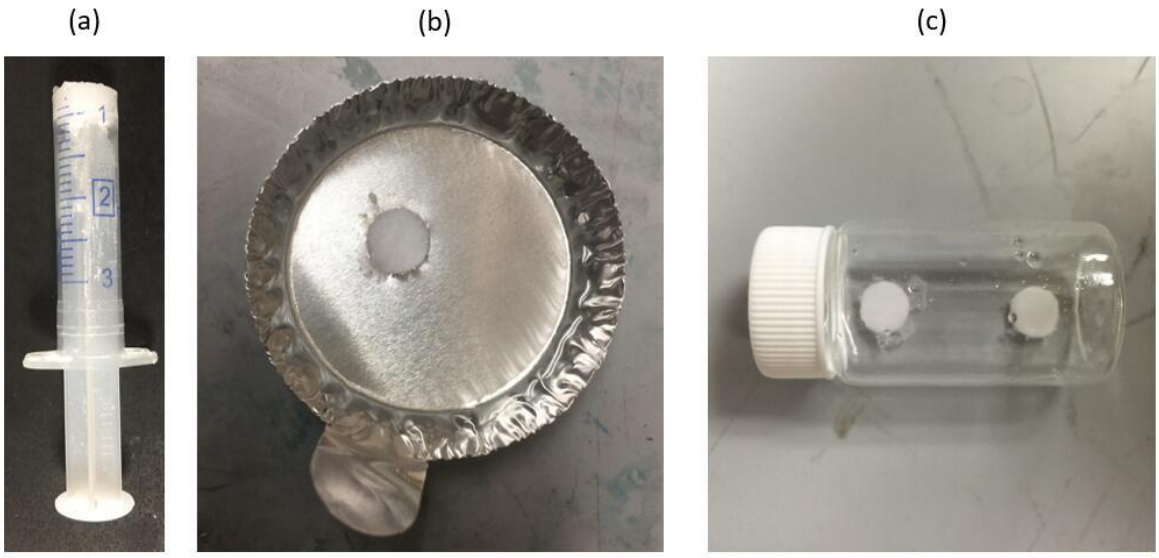

Figure 5.7 Cylindrical pellets of the mixture of GUR 2122 particles, glycol and oil. (a) Making pellet using a syringe with its front end cut off. (b) Pellet ejected using the plunger of the syringe then put into the foil pan containing glycol. (c) Pellets after sintering and washing.

Figure 5.8 shows the SEM images with low magnification of the binary phase-mixture of GUR 2122 particles/glycol with $\phi_p = 0.4$ (image (a)) and the ternary mixture of GUR 2122 particles/glycol/oil with the composition of glycol:oil:particle = 0.5:0.206:0.294 (image (b)); 0.5:0.25:0.25 (image (c)); 0.5:0.283:0.217 (image (d)) and 0.5:0.3:0.2 (image (e)), respectively. Figure 5.9 shows the same samples but at larger magnification (100x).

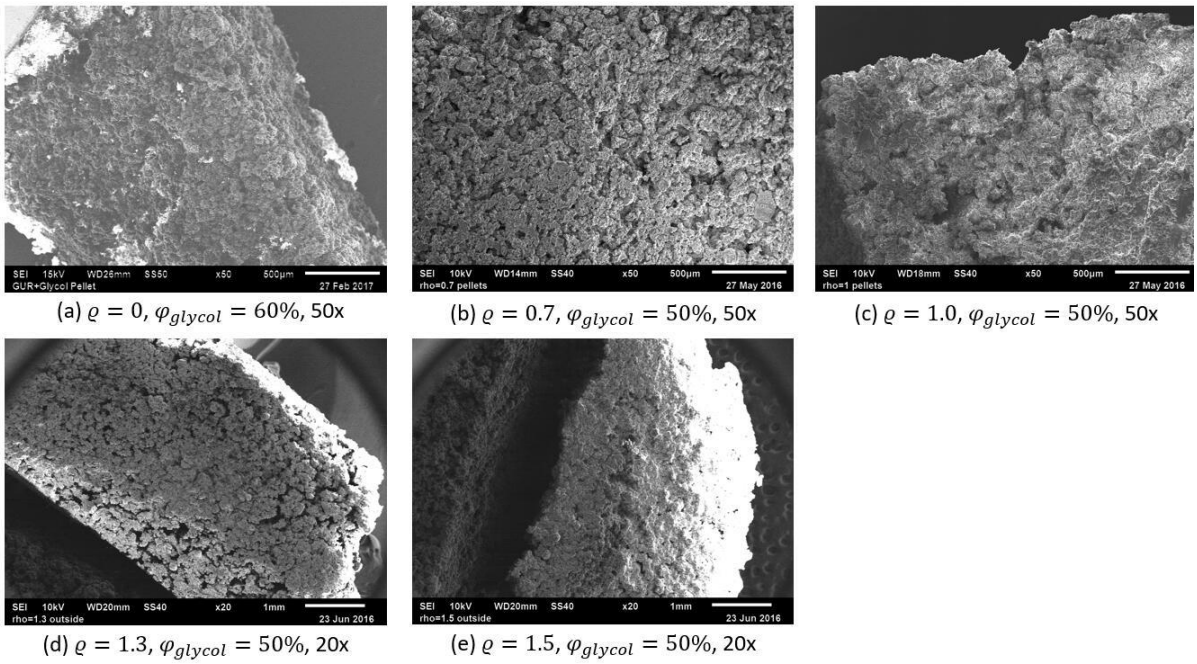

(a) $\varrho = 0$, $\varphi_{glycol} = 60\%$, 50x (b) $\varrho = 0.7$, $\varphi_{glycol} = 50\%$, 50x (c) $\varrho = 1.0$, $\varphi_{glycol} = 50\%$, 50x

(d) $\varrho = 1.3$, $\varphi_{glycol} = 50\%$, 20x (e) $\varrho = 1.5$, $\varphi_{glycol} = 50\%$, 20x

Figure 5.8 SEM images of pellets of (a) the mixture of GUR 2122 particle/glycol with $\boldsymbol{\varphi_{glycol} = 60\%}$, no oil added; (b) $\boldsymbol{\varphi_{glycol} = 50\%, \varrho = 0.7}$; (b)$\boldsymbol{\varphi_{glycol} = 50\%, \varrho = 1.0}$. (d) $\boldsymbol{\varphi_{glycol} = 50\%, \varrho = 1.3}$. (e) $\boldsymbol{\varphi_{glycol} = 50\%, \varrho = 1.5}$. The magnification of (a) (b) (c) is 50x, and the magnification of (d) (e) is 20x.

It is notable that when troweling the pellets by using spatula in the syringe with its front end cut off, small amount of liquid flowed out of the pellets. Thus, the composition of the pellet may be slightly different from the composition of the original mixture in the vial. For above three images, it can be recognized that all the five pellets, no matter if they are originally binary mixture of GUR 2122 particles and glycol or ternary mixture of GUR 2122 particles, glycol and oil, all have macro-porous structures and their textures took fairly similar.

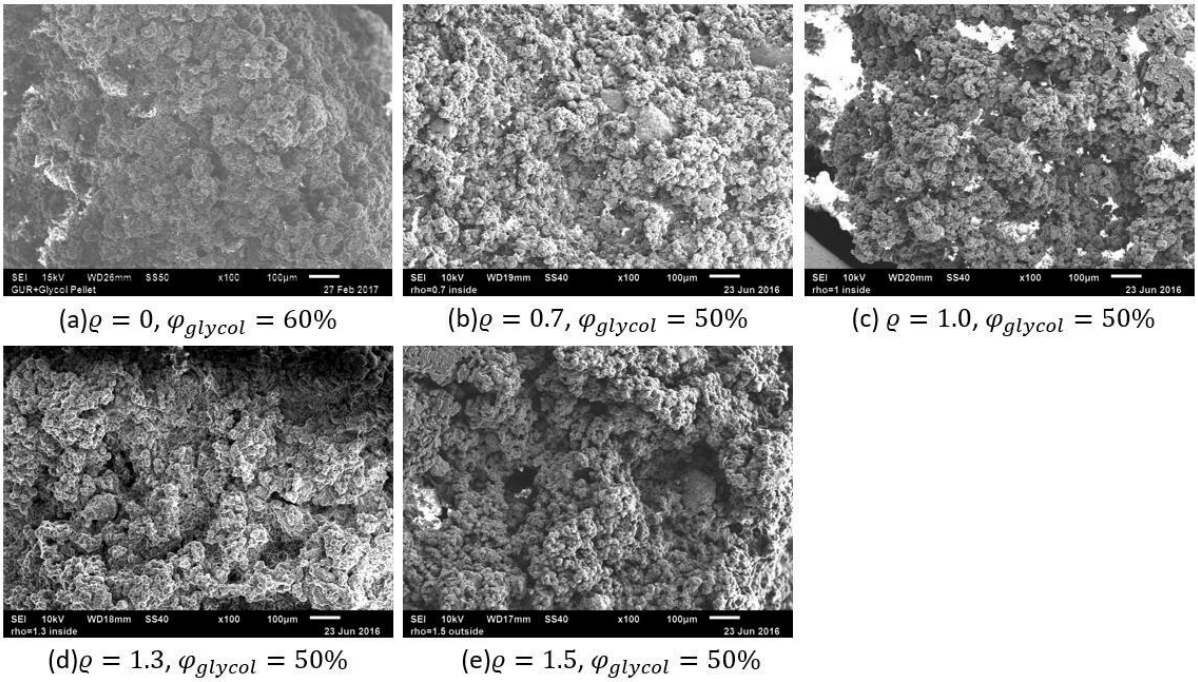

(a)$\varrho = 0, \varphi_{glycol} = 60\%$ (b)$\varrho = 0.7, \varphi_{glycol} = 50\%$ (c) $\varrho = 1.0, \varphi_{glycol} = 50\%$

(d)$\varrho = 1.3, \varphi_{glycol} = 50\%$ (e)$\varrho = 1.5, \varphi_{glycol} = 50\%$

Figure 5.9 SEM images of pellets of (a) the mixture of GUR 2122 particle/glycol with $\boldsymbol{\varphi_{glycol} = 60\%}$, no oil added; and the mixture of GUR 2122 particle/glycol/oil with $\boldsymbol{\varphi_{glycol} = 50\%}$, and (b) $\boldsymbol{\varrho = 0.7}$ (c) $\boldsymbol{\varrho = 1.0}$ (d) $\boldsymbol{\varrho = 1.3}$ (e) $\boldsymbol{\varrho = 1.5}$. For all the five images, the magnification is 100x.

Although when the ϱ value is larger than 1.3, separation occurred, the pellet can still be made by packing the mixture with a metal spatula. Obviously, the composition of pellet is different from the composition of original mixture in the vial. Moreover, the oil can be absorbed by the molten particles, so the composition may change during the sintering process. However, as the sintering time for GUR 2122 samples was just 10 minutes, although the temperature (150℃) is above the melting point, the particles were partially melting, and the portion of amorphous phase is not on a large scale. So the changes of composition of is not a big problem.

It is notable that for the samples which ϱ=1.3 and ϱ=1.5, the aggregates of particles still existed. At such high ϱ values, spherical particles such as Micropoly 250S would have been in a slurry state and the macro-porous structure would have collapsed. Moreover, the pore sizes and aggregate sizes of those five samples are very similar, although their composition are quite different. From this point, it can be concluded that the aggregates inside the pellets mostly corresponded to the initial "popcorn-like".

SEM images with even larger magnification i.e. 200x, 500x, and 1000x of the same samples on Figure 5.8 and Figure 5.9 have also been taken (not shown) and support the same conclusion.

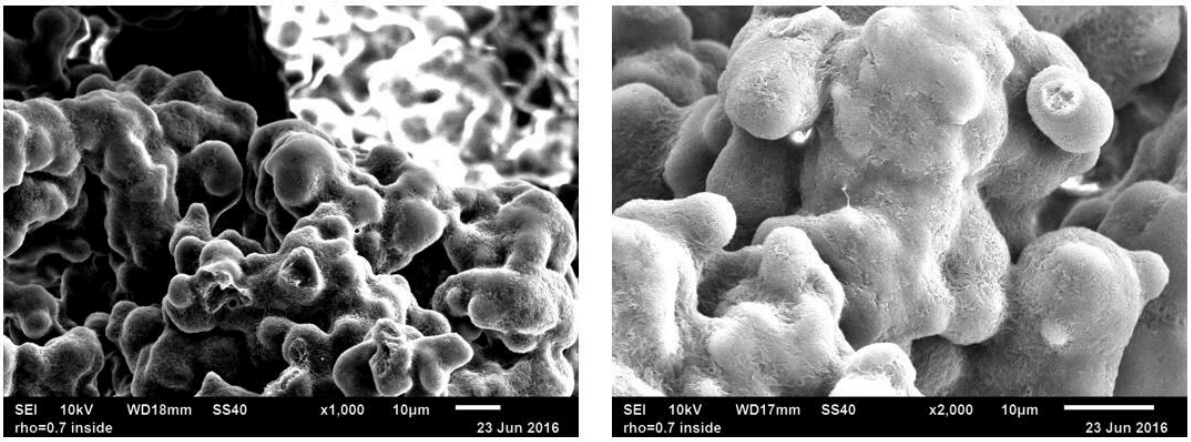

Figure 5.10 SEM images of inside pellets of the mixture of GUR 2122 particle/glycol/oil with $\boldsymbol{\varphi_{glycol} = 50\%}$, and $\boldsymbol{\varrho = 0.7}$, with the magnification of 1000 times (left) and 2000 times (right).

Figure 5.10 shows the SEM images of inside pellets at 1000 and 2000 times magnification. As we can see, GUR 2122 polyethylene particles were partially melting at the temperature as high as

150℃. The necks between the particles have clearly developed, in qualitative agreement with Frenkel's model. [41] This would also suggest some shrinkage of the porous network, however, we have not tried to quantify this.

5.4 EXTRUDATES OF THE GUR 2122 PARTICLE SAMPLES AFTER SINTERING AND WASHING

Extrudates of the mixture of GUR 2122 particles, glycol and oil were prepared by placing the sample into an intact syringe then extruding the sample out. As shown on Figure 5.11 (a) and (b), no needle was used on the syringe, and hence the diameter of the extrudates was the same as the exit hole of the syringe. Figure 5.11 (c) shows the extrudates after sintering and washing in water for 24 hours to remove glycol and in hexane for 24 hours to remove oil.

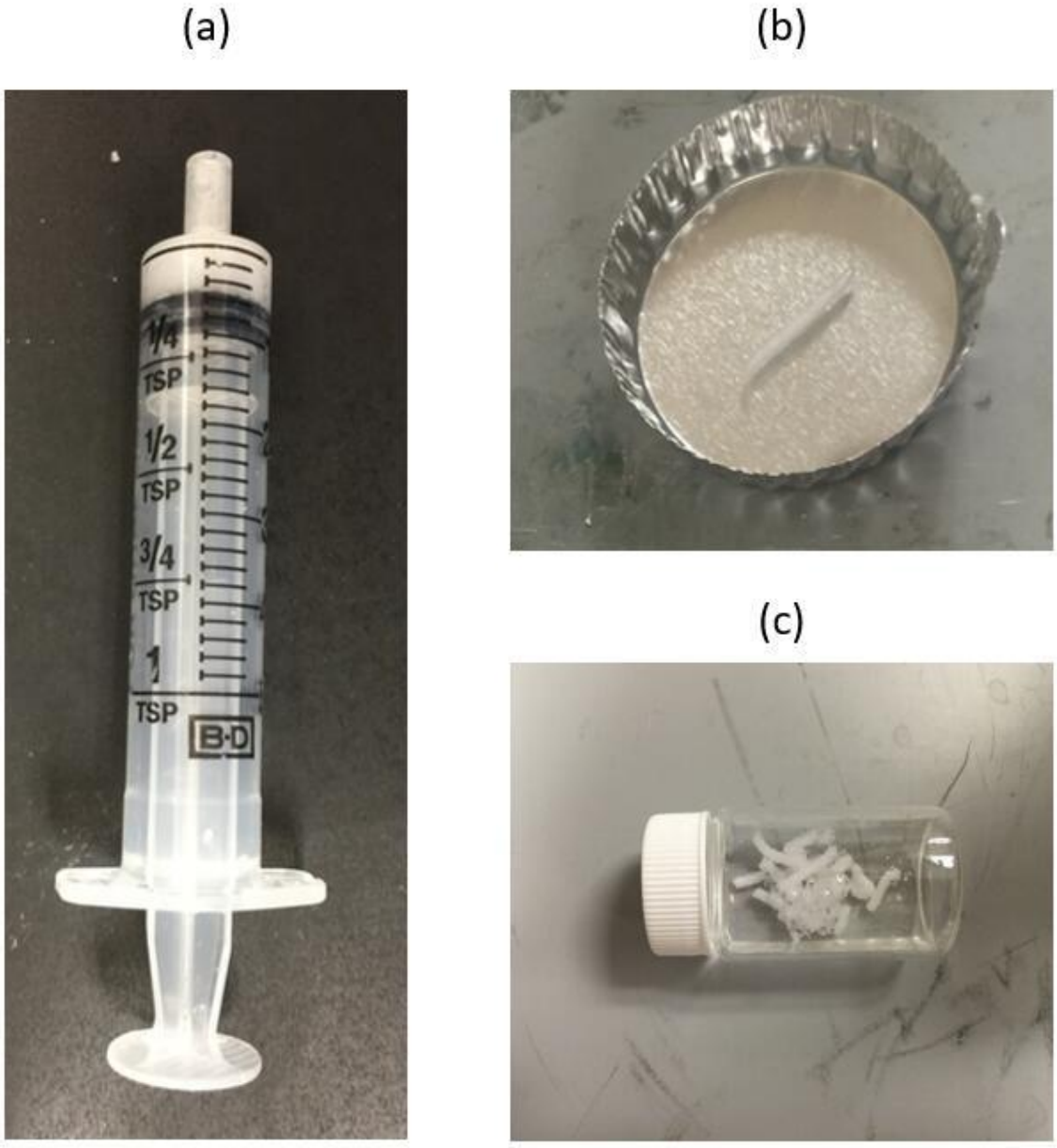

Figure 5.11 Extrudates of the mixture of GUR 2122 particles, glycol and oil. (a) Making extrudates using a syringe without needle. (b)Extrudates in a foil pan before sintering. (c) Extrudates after sintering and washing.

Figure 5.12 shows the low magnification SEM images of the extrudates of GUR 2122 particles samples with various composition of glycol and oil. If the ϱ value is sufficiently large (larger than 1.0), the samples were too dilute to be made as extrudates.

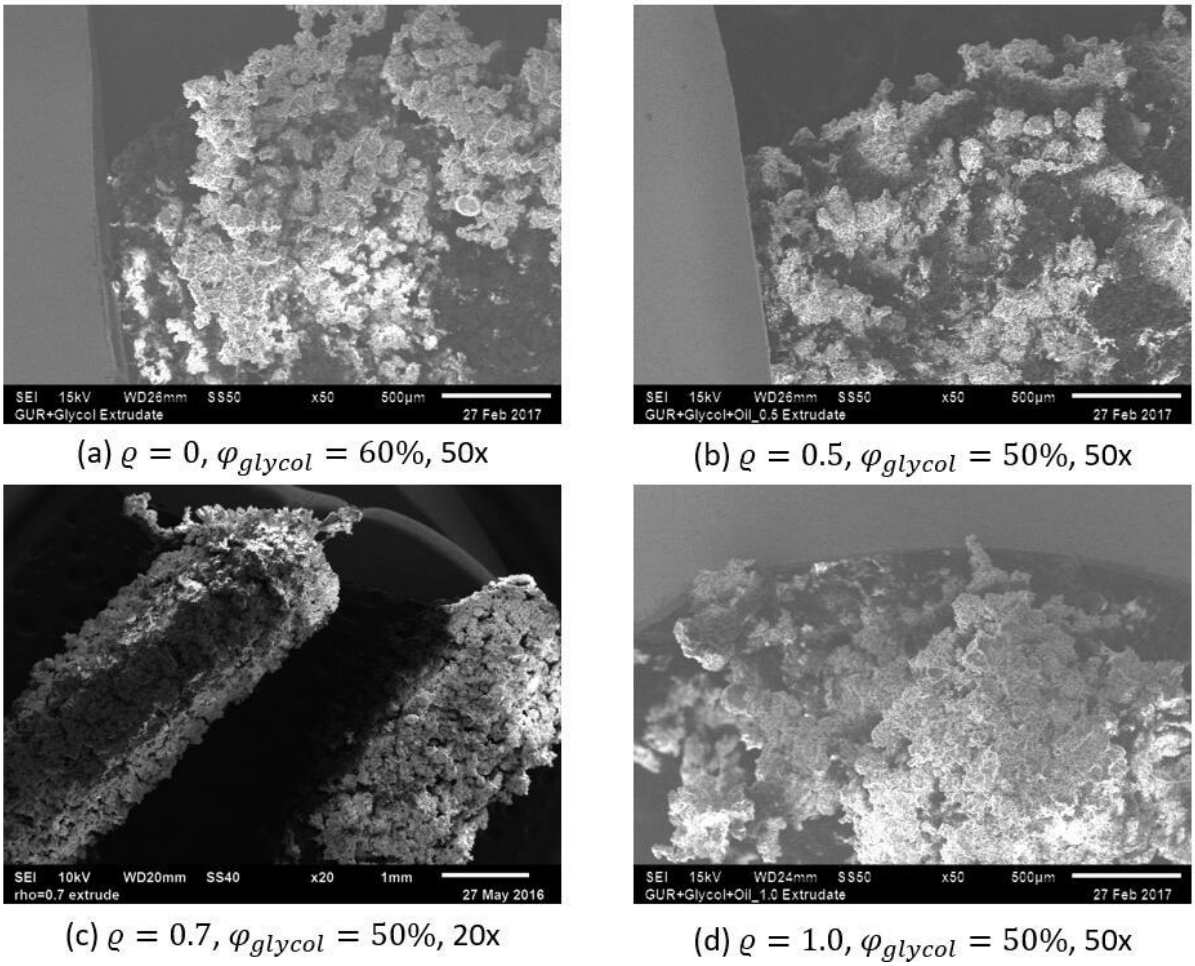

Figure 5.12 SEM images of extrudates of the mixture of (a) GUR 2122 particle/glycol, $\boldsymbol{\varphi_{glycol} = 60\%}$, no oil added, 50x magnification; (b) GUR 2122 particle/glycol/oil with $\boldsymbol{\varphi_{glycol} = 50\%}$ and $\boldsymbol{\varrho = 0.7}$, 50x magnification; (c) GUR 2122 particle/glycol/oil with $\boldsymbol{\varphi_{glycol} = 50\%}$ and $\boldsymbol{\varrho = 0.7}$, 20x magnification; and (d) GUR 2122 particle/glycol/oil with $\boldsymbol{\varphi_{glycol} = 50\%}$ and $\boldsymbol{\varrho = 1.0}$, 50x magnification.

As shown on Figure 5.12, although the composition of the extrudates are quite different, all the extrudates appeared to have a macro-porous structure.

Figure 5.13 shows the SEM images of the same samples on Figure 5.12 but at a larger magnification (200x).

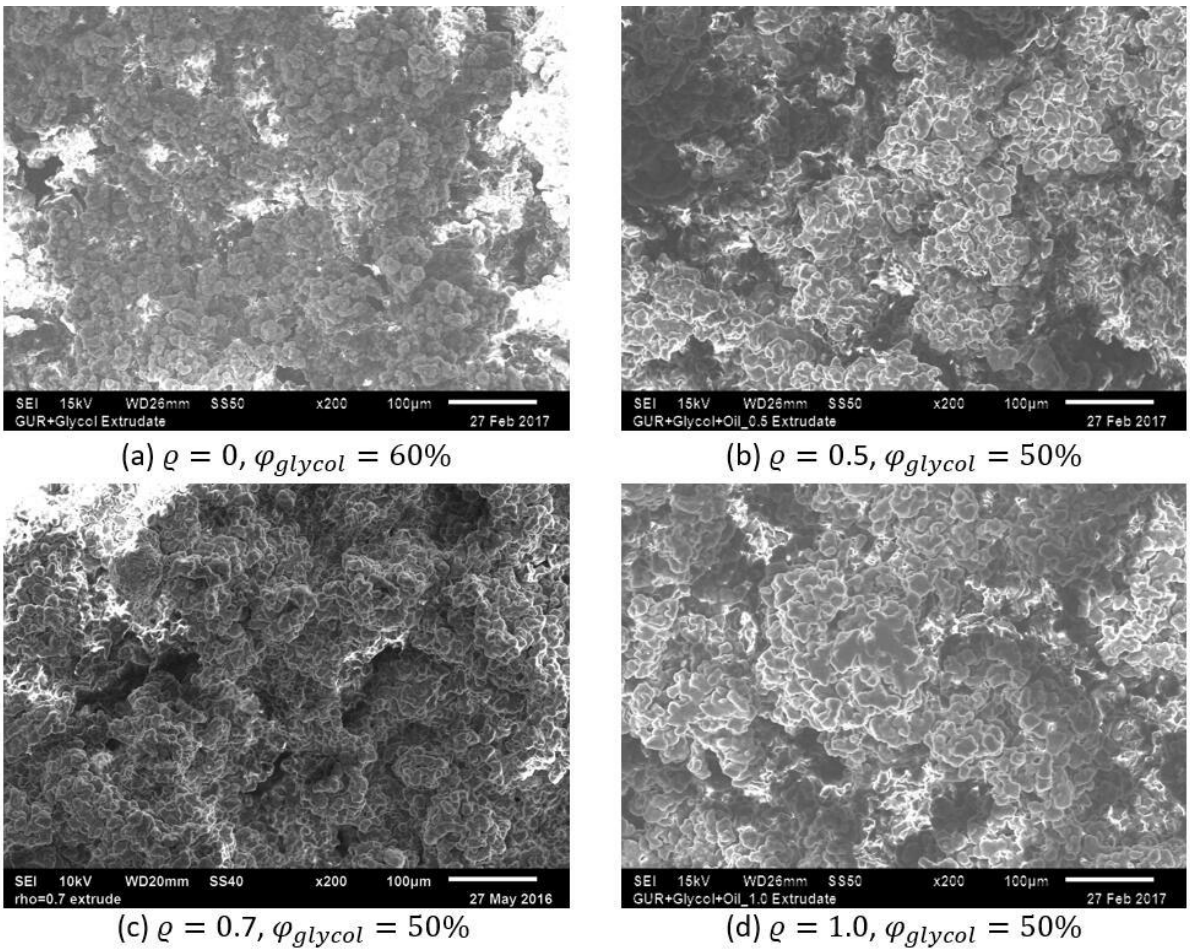

Figure 5.13 SEM images of extrudates of the mixture of (a) GUR 2122 particle/glycol, $\boldsymbol{\varphi_{glycol} = 60\%}$, no oil added; (b) GUR 2122 particle/glycol/oil with $\boldsymbol{\varphi_{glycol} = 50\%}$ and $\boldsymbol{\varrho = 0.7}$; (c) GUR 2122 particle/glycol/oil with $\boldsymbol{\varphi_{glycol} = 50\%}$ and $\boldsymbol{\varrho = 0.7}$; (d) GUR 2122 particle/glycol/oil with $\boldsymbol{\varphi_{glycol} = 50\%}$ and $\boldsymbol{\varrho = 1.0}$.

As shown on the images, it is clear that the composition of the mixture does not affect the size of pores and aggregates significantly. The same conclusion as mentioned on the results of pellets can be drawn that the initial "popcorn-like" aggregates of GUR 2122 particles worked as the building blocks of the macro-porous structure; this is different from capillary aggregate networks in which large aggregates form the building blocks of the network. The effect of the composition

of the mixture, i.e. the volume fraction of glycol or oil, on the size of pores and aggregates are not obvious.

Similar to the pellets, in the process of preparing extrudates, the composition of the mixtures may also be different from the composition of the original mixture in the vial.

5.5 RESULT ON CELLS GROWTH

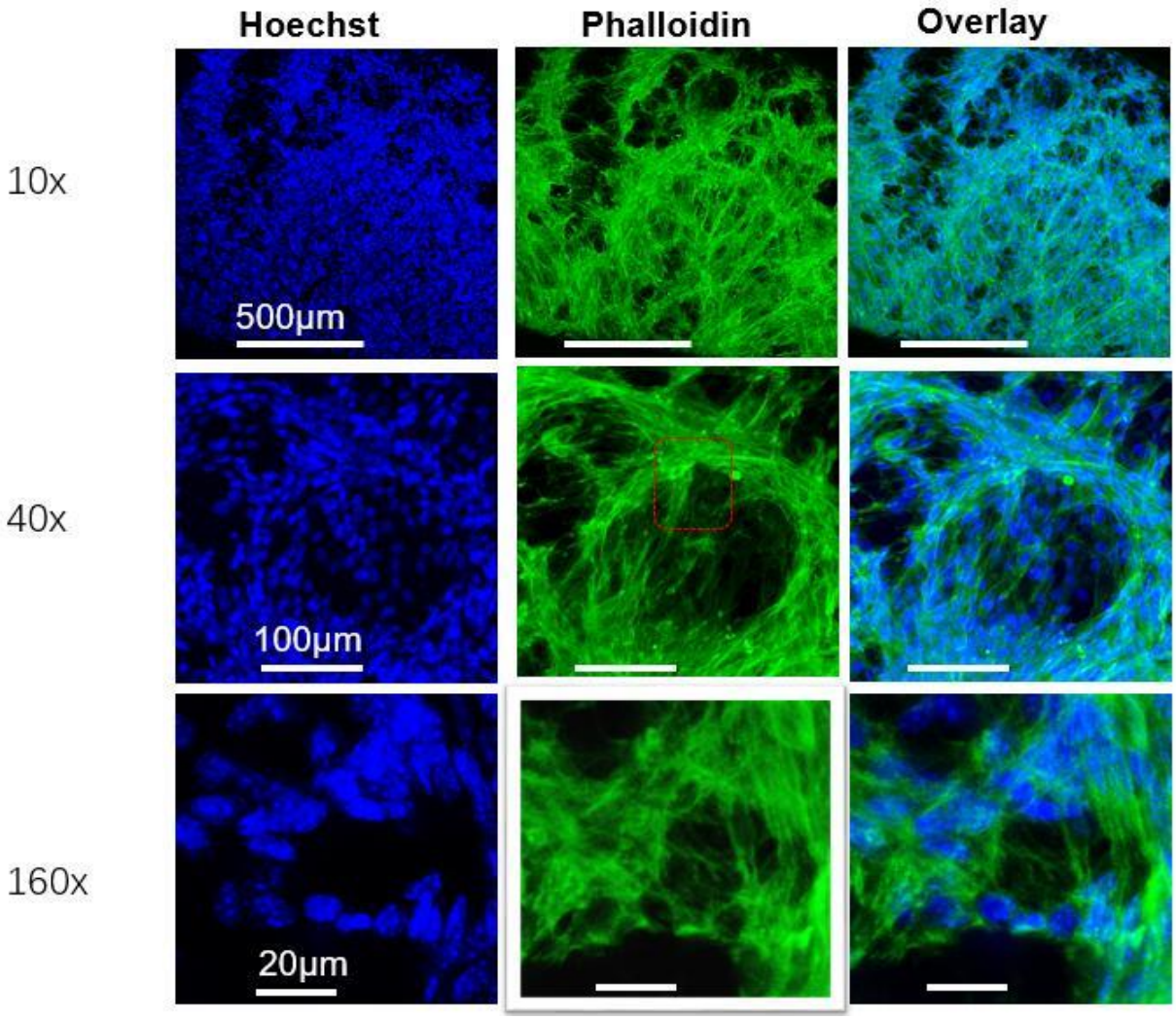

Figure 5.14 Sintered pellet of GUR 2122/glycol/oil using as scaffold for growing cells.

Figure 5.14 shows the sintered pellets ($\varphi_{glycol} = 50\%, \varrho = 0.7\ and\ 1.0, respectively$) can be used as scaffolds for cells growth. The cells used in the cells migration growth experiments are C1C12 mouse (skeletal muscle) cells.

The Hoechst is commonly used to stain DNA in bacteria or eukayote cells, which is excited by ultraviolet light at around 350 nm, and emits blue-cyan fluorescent light [42]. Since DNA is marked by the Hoechst dye, the cell nucleus and mitochondria can be recognized. [43] Phalloidin can tightly and selectively bind to F-actin, thus, derivatives of phalloidin containing fluorescent tags are used widely in microscopy to visualized F-actin in biomedical research. [44] The images of right column of Figure 5.14 shows the overlay of the images of the left and middle column.

As shown on Figure 5.14, the cells proliferate into the pores of the scaffold.

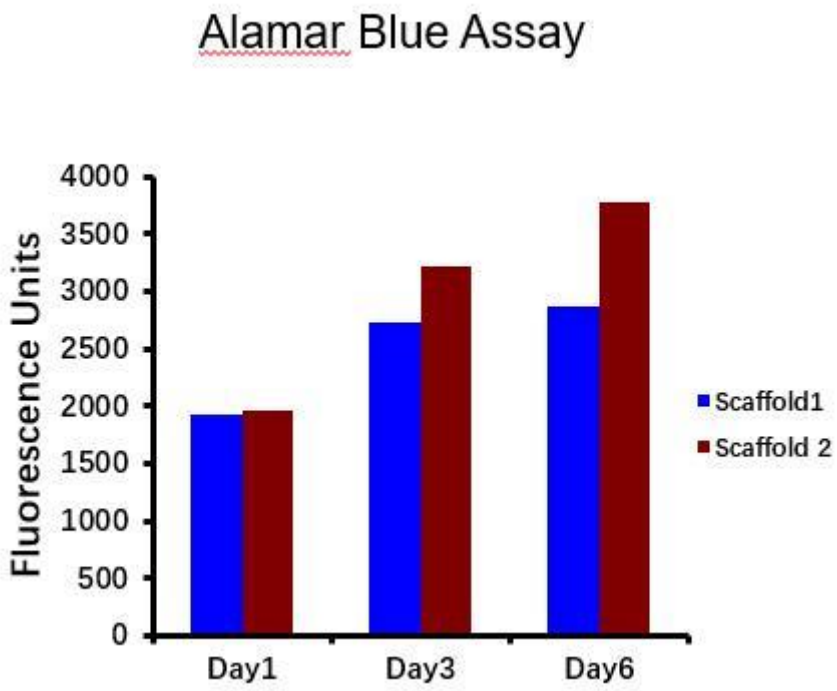

Figure 5.15 Fluorescence Units vs days of cells growing in the sintered pellets of GUR 2122 particle/glycol/oil.

Viability of the cells was examined by the Alamar Blue assay whose function has been described in Citation [45,46]. Alamar Blue cell viability reagent functions as a cell health indicator by using the reducing power of living cells to quantitatively measure the proliferation of the cells. We measured metabolic activity by alamarBlue assay that is based on the enzymatic reduction of resazurin to resorufin by nicotinamide adenine dinucleotide (NADH) dehydrogenase. When cells are alive they maintain a reducing environment within the cytosol of the cell. Resazurin, the active ingredient of alamarBlue reagent, is a non-toxic, cells permeable compound that is blue in color and virtually non-fluorescent. Upon entering cells, resazurin is reduced to resorufin, a compound that is red in color and highly fluorescent. Viable cells continuously convert resazurin to resorufin, increasing the overall fluorescence and color of the media to resorufin, increasing

the overall fluorescence and color of the media surrounding cells. [45,46] shows the fluorescence intensity increased with the number of days of cells growing in the pellets scaffold. Scaffold 1 here is the sintered pellet which $\varphi_{glycol} = 50\%,\ \varrho = 0.7$, and Scaffold 2 here is the sintered pellet which $\varphi_{glycol} = 50\%, \varrho = 1.0$.

All of the operation of this section were conducted by Dr.Manjulata Singh from the Medicine School of the University of Pittsburgh.

6.0 CONCLUSIONS

This study had three main goals, (1) implementing capillary aggregate networks in mixtures that are inverted as compared to our previous research, i.e. the continuous phase is aqueous and the particles are hydrophobic (polyethylene), (2) obtaining dry macro-porous material by sintering the inverted ternary system that mentioned above, and (3) using that porous material as a scaffold for growing cells.

Due to the high hydrophobicity of PE particles, it is impossible to maintain a stable suspension of PE particles in water, so we replaced water by ethylene glycol as the continuous phase. In the sintering process, the Micropoly 250S PE particles are much more sensitive to time and temperature than the ultrahigh molecular weight PE particles, GUR 2122, due to their low viscosity. To obtain the permanent sintered macro-porous material, the samples of Micropoly 250S particles can only be sintered at the temperature slightly lower than its melting point, i.e. 123℃, for a long time (4 hours) by using the oil bath. Increasing the volume fraction of oil leads to lower melting point of Micropoly 250S particles. The viscosity of molten Micropoly 250S particls is about 1.5 Pa · s. The viscosity of molten GUR 2122 particles, however, is much higher. Since it is unsuccessful even in molding discshaped GUR 2122 samples for rheological testing, the accurate viscosity of molten GUR 2122 particles cannot be measured.

Due to this high viscosity, for the samples of GUR 2122 particles, the sintering procedure is more forgiving: they can be sintered for long time at temperature far above their melting point without collapse. Since ternary mixtures based on GUR 2122 particles have much stronger structure prior to sintering compared to the samples of Micropoly 250S particles, they can be made as pellets and extrudates, and sintered in a glycol bath at 150℃ (which is at least 10℃ higher than the melting point of GUR 2122 particles) for 10 minutes. Another notable phenomenon is that particles may absorb the oil if the sintering time is long, and when the polymer recrystallized, the oil was simply retained in the amorphous portion of the semi-crystalline sample. We have not yet fully quantified this.

The optical microscopy shows that Micropoly 250S particles dispersed very well in the light mineral oil. Both optical microscopic images and SEM images demonstrated that at an appropriate volume fraction of glycol, e.g. 50%, by increasing the ϱ value, the size of capillary aggregates increased. Also, the pores size increased by increasing the ϱ value. Thus, it can be concluded that for the samples of Micropoly 250S particles, we can control the pores size by adjusting the ϱ value. In contrast, GUR 2122 particles do not disperse well in oil: they appeared as initial "popcorn-like" aggregates. Because of this, the effect of composition of mixtures on pore size is very limited. For instance, higher ϱ values did not lead to increased size of capillary aggregates, and therefore increased pore size. Instead, the aggregates appear to be on the same size scale as the original "popcorn-like" aggregates. Large magnification SEM images demonstrate the partially melting of the both kinds of particles.

The initial "popcorn-like" aggregates of GUR 2122 particles, binary mixture of particles and glycol can give strong pastes if the particle loading is at least 40%. However, the ternary

mixture of GUR 2122 particles, glycol and oil is already strong at 30% particle loading. This advantage allows pellets or extrudates be made at lower particle loading. Hence higher porosity can be obtained. Cells can grow well in the scaffold made of GUR 2122 particles, since the fluorescence which marked the organism that was secreted by the cells were observed and the fluorescence units increased from the first to the sixth day.

BIBLIOGRAPHY

[1] Velankar, S.S., *A non-equilibrium state diagram for liquid/fluid/particle mixtures*. Soft Matter, 2015. **11**: p.8393-8403.

[2] Domenech, T. and Velankar, S.S. *On the rheology of pendular gels and morphological developments in paste-like ternary systems based on capillary attraction*. Soft Matter, 2015. **11**(8): p.1500-1516

[3] Domenech, T. and Velankar, S.S. *Capillary-driven percolating networks in ternary blends of immiscible polymers and silica particles*. Rheologica Acta, 2014. **53**(8): p.1–13

[4] Cai, X.X., Li, B.P., Pan, Y. and Wu, G.Z. *Morphology evolution of immiscible polymer blends as directed by nanoparticle self-agglomeration.* Polymer, 2012. **53**(1): p.259–266.

[5] Lee, S. H., Bailly, M., and Kontopoulou, M., *Morphology and Properties of Poly(propylene)/Ethylene-Octene Copolymer Blends Containing Nanosilica.* Macromolecular Materials and Engineering, 2012. 297(1): p.95–103.

[6] Herminghaus, S., *Dynamics of wet granular matter*. Advances in Physics, 2005. **54**(3): p.221-261.

[7] Iveson, S.M., Lister, J.D., Hapgood, K. and Ennis, B.J, *Nucleation, growth and breakage phenomenon in agitated wet granulation processes: a review.* Powder Technology, 2001. **117**(3): p.3-39.

[8] Tarimala, S. and Dai, L.L., *Structure of microparticles in solidstabilized emulsions.* Langmuir, 2004. **20**(9): p.3492–3494.

[9] Tavacoli, J.W., Thijssen, J.H.J., Schofield A.B. and Clegg, P.S., *Novel, Robust, and Versatile Bijels of Nitromethane, Ethanediol, and Colloidal Silica: Capsules, SubTenMicrometer Domains, and Mechanical Properties*. Advanced Functional Materials, 2011. **21**(11): p.2020–2027.

[10] Koos, E. and Willenbacher, N., *Capillary Forces in Suspension Rheology*. Science, 2011. **331**(6019): p.897–900.

[11] Domenech, T and Velankar, S.S., *From hierarchical assembly to bicontinuous gels and microporous materials in polymer-polymer-particle three phase systems*. Department of Chemical Engineering, University of Pittsburgh. (Unpublished)

[12] Namiko, M. and Nori, F., *Wet granular materials*. Advances in Physics, 2006. **55**(1): p.1-45.

[13] Heidlebaugh, S.J., Domenech, T., Iasella, S.V. and Velankar, S.S., *Aggregation and separation in ternary particle/oil/water systems with fully wettable particles*. Langmuir, 2014. **30**(1): p.63-74.

[14] Binks, B.P., *Particles as surfactants - similarities and differences*. Current Opinion in Colloid & Interface Science, 2002. **7**(1-2): p.21-41.

[15] Walz, J.Y., *Colloidal Particles at Liquid Interfaces*. Journal of the American Chemical Society, 2007. **129**(13): p.4106-4107.

[16] Dickinson, E., *Food emulsions and foams: Stabilization by particles*. Current Opinion in Colloid & Interface Science, 2010. **15**(1-2): p.40-49.

[17] Horozov, T.S. and Binks, B.P. *Particle-stabilized emulsions: A bilayer or a bridging monolayer*, 2006. Angewandte Chemie, 2006. **45**(5): p.773-776.

[18] Thareja, P.; Velankar, S.S., *Particle-induced bridging in immiscible polymer blends*. Rheologica Acta, 2007. **46**(3): p.405-412.

[19] Thareja, P.; Velankar, S.S., *Rheology of immiscible blends with particle-induced drop clusters*. Rheologica Acta, 2008. **47**(2): p.189-200.

[20] Lee, M.N., Chan, H.K. and Mohraz, A., *Characteristics of Pickering Emulsion Gels Formed by Droplet Bridging.* Langmuir, 2012. **28**(6): p.3085-3091.

[21] Frost, D.S., Schoepf, J.J., Nofen, E.M. and Dai, L.L., *Understanding droplet bridging in ionic liquid-based Pickering emulsions.* Colloid Interface Science, 2012. **383**(1): p.103-109.

[22] Lee, M.N. and Mohraz, A. *Bicontinuous Macro-porous Materials from Bijel Templates*. Advanced Materials, 2010. **22**(43): p.4836-4841.

[23] Clegg, P.S., *Fluid-bicontinuous gels stabilized by interfacial colloids: low and high molecular weight fluids*. Journal of Physics: Condensed Matter, 2008. **20**(11): p.113101-113120.

[24] Tavacoli, J.W., Thijssen, J.H.J., Schofield, A.B. and Clegg, P.S., *Novel, Robust, and Versatile Bijels of Nitromethane, Ethanediol, and Colloidal Silica: Capsules, Sub-TenMicrometer Domains, and Mechanical Properties*. Advanced Functional Materials, 2011. **21**(11): p.2020-2027.

[25] Stratford, K., Adhikari, R., Pagonabarraga, I. and Desplat, J.C., *Cates, M. E. Colloidal jamming at interfaces: A route to fluidbicontinuous gels*. Science, 2005. **309**(5744): p.2198-2201.

[26] Bocquet, L., Charlaix, E., Ciliberto, S., and Crassous, J. *Moisture-induced ageing in granular media and the kinetics of capillary condensation*. Nature, 1998. **396**(6713): p.735-737.

[27] Willett, C.D., Adams, M.J., Johnson, S.A., and Seville J.P.K. *Capillary bridges between two spherical bodies*. Langmuir, 2000. **16**(24): p.9396-9405.

[28] Kralchevsky, P.A. and Nagayama, K., *Capillary Interactions between Particles Bound to Interface, Liquid Films and Biomembranes.* Advances in Colloid and Interface Science, 2000. **85**(2): p.145-192.

[29] Domenech, T., Yang, J., Heidlebaugh, S. and Velankar, S.S., *Three distinct open-pore morphologies from a single particle-filled polymer blend.* Physical Chemistry Chemical Physics, 2016. **18**(6): p.4310-4315.

[30] Capes, C.E. and Darcovich. K. *A survey of oil agglomeration in wet fine coal processing*. Powder Technology, 1984. **40**(1-3): p.43-52.

[31] Sirianni, A.F., Capes, C.E. and Puddington, J.E., *Recent experience with the spherical agglomeration process.* AlChE Journal, 1969. **47**(2): p.166-170.

[32] Sparks, B.D. and Meadus, F.W. *Spherical agglomeration in a conical drum*. The Canadian Journal of Chemical Engineering, 1977. **55**(5): p.502-505.

[33] House, C.I. and Veal, C.J. *Spherical agglomeration in minerals processing*. In Colloid and surface engineering: Applications in the process industries; Williams, R.A., Ed; Butterworth Heinemann: Oxford, 1992.

[34] Boode, K. and Walstra, P., *Partial Coalescence in Oil-in-Water Emulsions. 1. Nature of the Aggregation*. Colloids and Surfaces A: Physicochemical and Engineering Aspects, 1993. **83**: p.121-137.

[35] Pawar, A.B., et al., *Arrested coalescence of viscoelastic droplets with internal microstructure.* Faraday Discussions, 2012. **158**: p.341-350.

[36] Caggioni, M., et al., *Interfacial stability and shape change of anisotropic endoskeleton droplets*. Soft Matter, 2014. **10**(38): p.7647-7652.

[37] Gao, P. and Mackley, M.R., *A general model for the diffusion and swelling of polymers and its application to ultra-high molecular mass polyethylene*. Proc Roy Soc, 1994. **444**(1921): p.267-285。

[38] Wu, J.J., Buckley, C.P., and O'Connor, J.J., *Processing of ultra-high molecular weight polyethylene: modelling the decay of fusion defects*. Trans I Chem E Part A, 2002. **80**: p.423-431.

[39] Hambir, S. and Jog, J.P., *Sintering of ultra hgh molecular weight polyethylene*. Bulletin of Materials Science, 2000. **23**(3): p.221-226.

[40] Torres, F.G., Cubillas, M.L. and Quintana, O.A. *Sintering of non-spherical polyethylene particles*. Polymer and Polymer Composites, 2006. **14**(5): p.503-513.

[41] Frenkel, J. *Viscous flow of crystalline bodies under the action of surface tension*. Journal of Physics, 1945. **9**(5): p.385-391.

[42] Latt, S.A. and Stetten, G., *Spectral studies on 33258 Hoechst and related bisbenzimidazole dyes useful for fluorescent detection of deoxyribonucleic acid synthesis*. Journal of Histochemistry and Cytochemistry, 1976. **24**(1): p.24-33.

[43] Latt, S.A., et al, *Recent developments in the detection of deoxyribonucleic acid synthesis by 33258 Hoechst fluorescence*. Journal of Histochemistry and Cytochemistry, 1975. **23**(7):p.493-505.

[44] George, P.R., **Phalloidin**. Encyclopedia of Genetics, Genomics, Proteomics and Informatics, 2008. **2**: p.1475.

[45] https://www.thermofisher.com/us/en/home/references/protocols/cell-and-tissueanalysis/cell-profilteration-assay-protocols/cell-viability-with-alamarblue.html

[46] Anoopkumar-Dukie, S. et al, *Resazurin assay of radiation response in cultured cells*. British Journal of Radiology, 2005. **78**(934): p.945-947.